

Acta Astronautica

Active space debris removal by ion multi-beam shepherd spacecraft

--Manuscript Draft--

| | |
|-------------------------------|---|
| Manuscript Number: | AA-D-22-01510R1 |
| Article Type: | Research paper |
| Section/Category: | Space Technology & Systems Development |
| Keywords: | space debris; ion beam; attitude motion; control law; contactless transportation; ion multi-beam shepherd |
| Corresponding Author: | Vladimir Aslanov Samara National Research University Samara, Russian Federation |
| First Author: | Vladimir Aslanov |
| Order of Authors: | Vladimir Aslanov Alexander Ledkov |
| Abstract: | <p>Contactless transportation of a passive object by an ion beam generated by an active spacecraft's thruster is the promising way of space debris removal. The study proposes a modification of the ion beam shepherd concept based on the using an array of impulse transfer thrusters. The multi-beam scheme allows to significant increase the generated ion force, which reduces a space debris object deorbit time, thereby reducing the probability of its collision with other orbital objects. The aim of the work is to study the possibility of using several ion beams for effective contactless transportation of a space debris object. Controlling the angular motion of the object allows to transfer it to the angular mode, in which the generated ion force is maximum. The article proposes a control law for impulse transfer thrusters, which is based on the calculation of the energy of the object's unperturbed motion, and two control schemes that implement this law: relay control, which implies turning the thruster on and off, and ion beam axis direction control for one of the thrusters. For a space debris object of a cylindrical shape, a comparison of the time and fuel costs required for deorbiting the object using one, two, and three impulse transfer thrusters is made. It is shown that the addition of thrusters significantly reduces the descent time, but has little effect on the mass of required fuel. For the case of two engines, the best angle of ion beams axes direction and the most angular motion mode are determined. Numerical simulation of space debris removal is carried out for the case when the space debris object is in the least favorable mode of angular motion and the proposed control schemes are used. The ion beam direction control scheme showed better results than the relay scheme. The use of multiple ion beams opens up new possibilities for creating new ion beam shepherd spacecraft design and developing new control methods and laws.</p> |
| Suggested Reviewers: | Claudio Bombardelli claudio.bombardelli@upm.es Mario Merino mario.merino@uc3m.es Matthew Cartmell m.cartmell@sheffield.ac.uk |
| Opposed Reviewers: | |
| Response to Reviewers: | <p>Dear Reviewers,</p> <p>The authors would like to thank you for valuable advice and recommendations, which made it possible to eliminate annoying typos and made the text more readable and clearer. All changes made to the text are marked in red.</p> <p>Review 1 Comment 1. "The abstract had some awkward English ..." Response 1. Thank you! We have made the recommended changes to the abstract.</p> <p>Comment 2. Won't the plasma environment in LEO require very close proximity to</p> |

work? In addition, won't the plasma environment change significantly during periods of increased solar activity?

Response 2. The following explanation was added to the introduction to the assumptions block. "According to the simulation results given in [29], the effect of the plasma environment on the value of the transferred ion force is negligible, since ion beam acts as potential barriers for the ambient plasma ions."

Comment 3. I think that the proposed distance between transportation system and derelict is 15m, is that correct?

Response 3. You are right. Clarification added to the beginning of Section 3.1 "The control system of the active spacecraft keeps it in the relative position , , so the distance between the transportation system and the space debris is 15m."

Comment 4. Won't there need to be some significant efforts to keep that distance constant?

Response 4. Distance maintained by control (6), (7). The mass costs calculated using equation (17) and given in Table 5 take into account the costs of maintaining a distance. The following explanation was added to the Discussion section: "The values given in the mass column include the cost of the impulse transfer thrusters, the impulse compensation thrusters and the control engines."

Comment 5. The diameter of the beam width as a function of distance from the shepherd will be important (it seems) but it was never mentioned. There was also no mention of the proposed beam width relative to the size of the derelict object - that seems to be an important ratio.

Response 5. This is a part of the calculation procedure given in [33]. The beam diameter can be found using the divergence angle given in Table 2. The following explanation was added before (17): "The diameter of the ion beam at the center of mass of space debris in the case of one thruster is 5.29 m. The ratio of beam diameter to the stage length is 1.39."

Comment 6. It was also in clear to me if the relationship between the tug and the derelict was in-track? It makes sense that the impulse you want to give to the derelict is basically a retrograde impulse.

Response 6. The following explanation was added before (17). "The use of control laws (6)-(7) requires tracking the relative position and relative velocity of the active spacecraft."

Comment 7. Engineering/operations - What is the size of the shepherd? The size of this spacecraft must be considered in the risk calculations. Can this device perform collision avoidance maneuvers while "shepherding" a derelict from orbit? Having three thrusters (vice one) will require a much larger solar array, this needs to be considered in the tradeoffs.

Response 7. Development of spacecraft design taking into account possible risks is beyond the scope of this study. However, we have expanded the paragraph in the Discussion that begins with "Calculations shown that the use of additional thrusters..." by adding a discussion of spacecraft size factors and the need for collision avoidance maneuvers.

Comment 8. just above equation, there is reference to "the blown body". Is that a typo? I am not sure what "blown" means.

Response 8. It's a typo. We removed the word "blown" from the phrase.

Comment 9. A few paragraphs before Fig 8, there is an equation stating " $r_0=7037400\text{km}$ " I suspect you mean " 7037400m "...???

Response 9. Thank you. It is typo. 7037400m is correct.

Review 2

Comment. I have only minor editorial comments, indicated on the attached revised copy of the manuscript.

Response. Thank you! All recommended edits have been made to the text.

The article is devoted to the actual topic of contactless space debris removal. The study proposes a modification of the ion beam shepherd concept based on the using an array of impulse transfer thrusters. The multi-beam scheme allows to significant increase the generated ion force, which reduces a space debris object deorbit time, thereby reducing the probability of its collision with other orbital objects. A numerical analysis of the multi-thruster scheme has been carried out and new schemes for controlling the angular position of space debris have been proposed. The use of multiple ion beams opens up new possibilities for shepherd spacecraft design and developing new control methods and laws.

Dear Reviewers,

The authors would like to thank you for valuable advice and recommendations, which made it possible to eliminate annoying typos and made the text more readable and clearer. All changes made to the text are marked in red.

Review 1

Comment 1. “The abstract had some awkward English ...”

Response 1. Thank you! We have made the recommended changes to the abstract.

Comment 2. Won't the plasma environment in LEO require very close proximity to work? In addition, won't the plasma environment change significantly during periods of increased solar activity?

Response 2. The following explanation was added to the introduction to the assumptions block. “According to the simulation results given in [29], the effect of the plasma environment on the value of the transferred ion force is negligible, since ion beam acts as potential barriers for the ambient plasma ions.”

Comment 3. I think that the proposed distance between transportation system and derelict is 15m, is that correct?

Response 3. You are right. Clarification added to the beginning of Section 3.1 “The control system of the active spacecraft keeps it in the relative position $x = 0$, $y = 15\text{m}$, so the distance between the transportation system and the space debris is 15m.”

Comment 4. Won't there need to be some significant efforts to keep that distance constant?

Response 4. Distance maintained by control (6), (7). The mass costs calculated using equation (17) and given in Table 5 take into account the costs of maintaining a distance. The following explanation was added to the Discussion section: “The values given in the mass column include the cost of the impulse transfer thrusters, the impulse compensation thrusters and the control engines.”

Comment 5. The diameter of the beam width as a function of distance from the shepherd will be important (it seems) but it was never mentioned. There was also no mention of the proposed beam width relative to the size of the derelict object - that seems to be an important ratio.

Response 5. This is a part of the calculation procedure given in [33]. The beam diameter can be found using the divergence angle given in Table 2. The following explanation was added before (17): “The diameter of the ion beam at the center of mass of space debris in the case of one thruster is 5.29 m. The ratio of beam diameter to the stage length is 1.39.”

Comment 6. It was also in clear to me if the relationship between the tug and the derelict was in-track? It makes sense that the impulse you want to give to the derelict is basically a retrograde impulse.

Response 6. The following explanation was added before (17). “The use of control laws **Error! Reference source not found.-Error! Reference source not found.** requires tracking the relative position and relative velocity of the active spacecraft.”

Comment 7. Engineering/operations - What is the size of the shepherd? The size of this spacecraft must be considered in the risk calculations. Can this device perform collision avoidance maneuvers while "shepherding" a derelict from orbit? Having three thrusters (vice one) will require a much larger solar array, this needs to be considered in the tradeoffs.

Response 7. Development of spacecraft design taking into account possible risks is beyond the scope of this study. However, we have expanded the paragraph in the Discussion that begins with "Calculations shown that the use of additional thrusters..." by adding a discussion of spacecraft size factors and the need for collision avoidance maneuvers.

Comment 8. just above equation, there is reference to "the blown body". Is that a typo? I am not sure what "blown" means.

Response 8. It's a typo. We removed the word "blown" from the phrase.

Comment 9. A few paragraphs before Fig 8, there is an equation stating " $r_0=7037400\text{km}$ " I suspect you mean " 7037400m "...???

Response 9. Thank you. It is typo. 7037400m is correct.

Review 2

Comment. I have only minor editorial comments, indicated on the attached revised copy of the manuscript.

Response. Thank you! All recommended edits have been made to the text.

Highlights

Modification of ion beam shepherd concept using an array of impulse transfer thrusters is proposed.

A control law for impulse transfer thrusters and two control schemes that implement this law are proposed.

Controlling the angular motion of a space debris object makes it possible to reduce fuel costs of a removal mission.

The use of multiple ion beams opens up new possibilities for shepherd spacecraft design and developing new control methods and laws.

Declaration of interests

The authors declare that they have no known competing financial interests or personal relationships that could have appeared to influence the work reported in this paper.

Active space debris removal by ion multi-beam shepherd spacecraft

A.S. Ledkov¹, V.S. Aslanov^{2,*}

Samara National Research University, Theoretical Mechanics Department,
Samara, Russia

Abstract

Contactless transportation of a passive object by an ion beam generated by an active spacecraft's thruster is a promising way of space debris removal. The study proposes a modification of the ion beam shepherd concept using an array of impulse transfer thrusters. The multi-beam scheme provides significant increase the generated ion force, which reduces a space debris object deorbit time, thereby reducing the probability of its collision with other orbital objects. The aim of the work is to study the possibility of using several ion beams for effective contactless transportation of a space debris object. Controlling the angular motion of the object permits orientation of the object to maximize the generated ion force. The article proposes a control law for impulse transfer thrusters, which is based on the calculation of the energy of the object's unperturbed motion, and two control schemes that implement this law: (1) relay control, which implies turning the thruster on and off, and (2) ion beam axis direction control for one of the thrusters. For a space debris object of a cylindrical shape, a comparison of the time and fuel costs required for deorbiting the object using one, two, and three impulse transfer thrusters is made. It is shown that the addition of thrusters significantly reduces the descent time, but has little effect on the mass of required fuel. For the case of two engines, the best angle of ion beams axes direction and the most preferable angular motion mode are determined. Numerical simulation of space debris removal is carried out for the case when the space debris object is in the least favorable mode of angular motion and the proposed control schemes are used. The ion beam direction control

¹ E-mail address: ledkov@inbox.ru. Website: <http://www.ledkov.com>

* Corresponding author

² E-mail address: aslanov_vs@mail.ru. Website: <http://aslanov.ssau.ru>

scheme showed better results than the relay scheme. The use of multiple ion beams opens up new possibilities for creating new ion beam shepherd spacecraft design and developing new control methods and laws.

Keywords: space debris; ion beam; attitude motion; control law; contactless transportation; ion multi-beam shepherd

1. Introduction

The threat of space debris is one of the challenges facing modern practical astronautics. Scientists agree that the solution to this problem is not possible without active space debris removal, which consists in the use of active spacecraft to deorbit large space debris or to transport it to a disposal orbit. Since the beginning of space activities, the amount of space debris in Earth orbit has been increasing. Maintaining the existing approaches to the problem, the population of space debris will grow at an accelerated rate [1]. According to the estimates given in [2,3], it is necessary to remove at least 5 large space debris objects annually to stabilize the situation in orbit. Given the plans of commercial companies to deploy their constellations of satellites, this number should be increased [4]. Study [5] provides a list of the most dangerous space debris objects in low Earth orbit (LEO). Over the past two decades, the scientific community has proposed many different schemes, approaches and methods for large space debris removal. Review articles [6–10] provide insight into the current state of affairs in this area. One of the promising ways of space debris removal is contactless transportation by means of an ion beam created by the thruster of an active spacecraft. Particles of the plume of the thruster hit a space debris surface and generate a force. This force can be used for transportation purposes. This idea has been proposed independently by three groups of scientists [11–13]. The force that is generated in such way will be referred to as the ion force. The absence of direct mechanical contact between the active spacecraft and the space debris object makes this method safe, since the risk of an accident during capture or

docking is excluded, and insensitive to the angular motion parameters of the space debris object, which makes it possible to transport even rapidly rotating objects.

To date, there are a lot of works devoted to various aspects of contactless ion beam assisted transportation of space debris. Mathematical models describing the motion of space debris and an active spacecraft during the space debris removal mission in various assumptions are developed in works [14,15]. The control laws of the active spacecraft relative position are proposed in [14,16–19]. Ion beam control laws for space debris motion relative to its center of mass are developed in research [20,21]. Space debris detumbling using ion beam torque is considered in [22,23]. Studies [24–26] are devoted to planning a missions of ion beam assisted space debris removal. Features of the physics of the ion beam and its interaction with the surface of space debris are studied in works [27–29]. A detailed analysis of studies on the topic of ion beam assisted transportation can be found in Section 4.2 of the review paper [10].

One of the weak points of contactless transportation by ion beam is the relatively small value of the generated force. The low value of the ion force leads to the fact that the transportation takes quite a long time. This can increase the probability of a transported object colliding with space debris when passing through densely populated heights. According to existing guidelines [30], the descent of space debris to Earth should not pose an undue risk to people or property. Deorbiting large space debris from LEO involves a controlled re-entry, for which the generated ion force may not be large enough. The magnitude of this force can be increased by increasing the ion outflow velocity or its concentration, which will require the modernization of the used ion engines. The article proposes a modification of the ion beam shepherd concept, which consists in the simultaneous use of several ion beams generated by different thrusters. In addition to increasing the generated force, the use of several beams creates additional opportunities for controlling the attitude motion of the transported object. Research [31] showed that controlling the object's angular motion during its contactless transportation can increase the efficiency of the system by transporting the object in an angular mode corresponding to the

maximum generated ion force. It should be noted that the use of several ion thrusters to generate an ion beam was described in [24], where a large space debris reorbiting mission in GEO was simulated using an active spacecraft equipped with four thrusters.

The aim of the work is to study the possibility of using several ion beams for effective contactless transportation of a space debris object. A comparison of a space debris object removal from LEO using one, two and three thrusters (Fig. 1) will be made. A control law that ensures the transfer of a space debris object to a given angular motion mode will be proposed. Two schemes for controlling the active spacecraft's thrusters that implement the developed control law will be considered. An estimation of the savings in time and fuel when using angular motion control during the space debris object descent will be made.

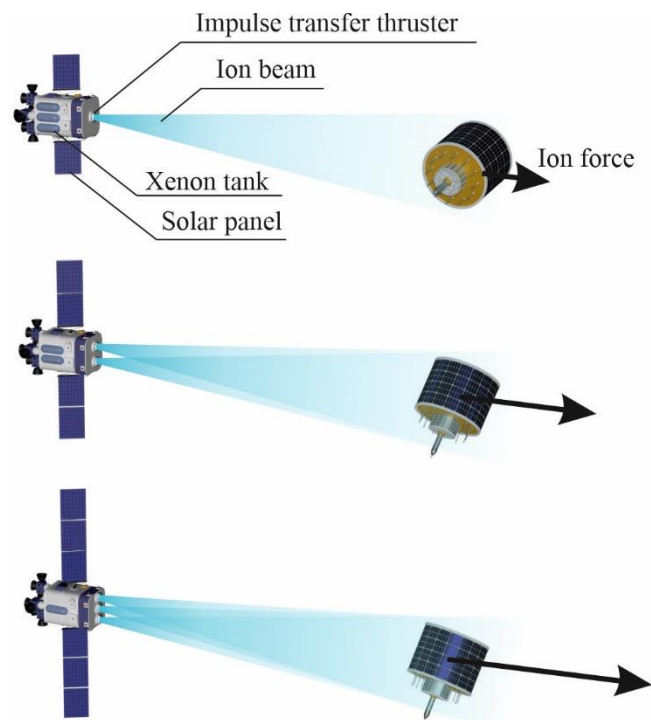


Fig. 1. Various active spacecraft designs.

During the study, several assumptions are made: the planar motion of the system is considered. It is assumed that the mutual influence of particles of intersecting ion beams is negligible due to the low concentration of particles in the plume and the high speed of their propagation. According to the simulation results

given in [29], the effect of the plasma environment on the value of the transferred ion force is negligible, since ion beam acts as potential barriers for the ambient plasma ions. The active spacecraft is considered as a material point, and the space debris object as a cylinder, the symmetry axis of which lies in the plane of the orbit. The center of mass of the cylinder is in its geometrical center. The motion occurs under the influence of only gravitational and ion forces and torques, as well as the thrust force of the control engines of the active spacecraft.

2. Mathematical model

2.1. Equations of motion

Consider the motion of a mechanical system consisting of a space debris object and an active spacecraft equipped with multiple impulse transfer thrusters, impulse compensation thrusters and control engines (Fig. 2). The equations of motion of the mechanical system do not differ from the conventional equations used to describe the motion of a system with a single ion impulse transfer thruster [32].

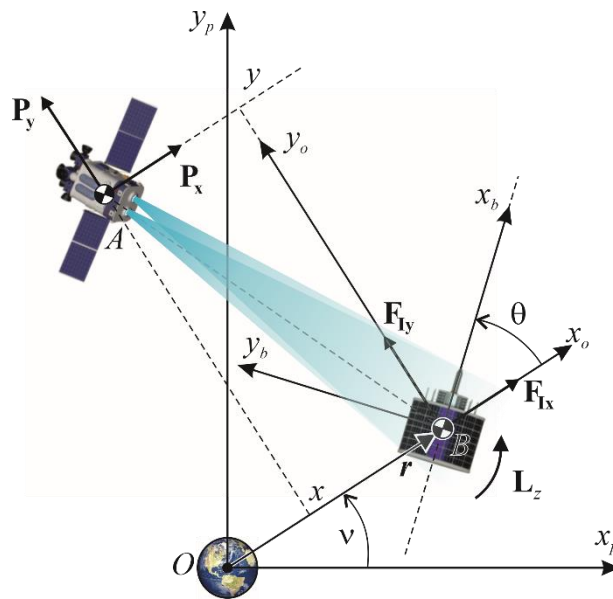


Fig. 2. Considered mechanical system.

$$\ddot{r} = \dot{\nu}^2 r - \frac{\mu}{r^2} + \frac{F_{tx}}{m_B} + \frac{3\mu(3I_x \cos^2 \theta + 3I_y \sin^2 \theta - I_x - I_y + I_z)}{2m_B r^4}, \quad (1)$$

$$\ddot{v} = -\frac{2\dot{v}\dot{r}}{r} + \frac{F_{Iy}}{m_B r} - \frac{3\mu(I_x - I_y)\sin\theta\cos\theta}{m_B r^5}, \quad (2)$$

$$\ddot{\theta} = \frac{L_z}{I_z} + \frac{2\dot{v}\dot{r}}{r} - \frac{F_{Iy}}{m_B r} + \frac{3\mu(I_x - I_y)\sin\theta\cos\theta}{r^3} \left(\frac{1}{m_B r^2} + \frac{1}{I_z} \right), \quad (3)$$

$$\ddot{x} = \ddot{v}y - \ddot{r} + \dot{v}^2(r+x) + 2\dot{v}\dot{y} + \frac{P_x}{m_A} - \frac{\mu(r+x)}{r_A^3}, \quad (4)$$

$$\ddot{y} = \dot{v}^2 y - \ddot{v}(r+x) - 2\dot{v}(\dot{r} + \dot{x}) + \frac{P_y}{m_A} - \frac{\mu y}{r_A^3}. \quad (5)$$

where r is the space debris object position vector, r_A is the distance between the active spacecraft and the center of the Earth, v is the true anomaly angle, θ is the space debris axis deflection angle, x, y are the active spacecraft's coordinates in Local-vertical/local-horizontal reference frame (LVLH). The origin of this frame coincides with the center of mass of the space debris object (point B). The axis Bx_o is directed along \mathbf{r} , the axis By_o is perpendicular to Bx_o and directed to the orbital flight direction, m_A is the mass of the active spacecraft, m_B is the mass of the space debris, I_x, I_y , and I_z are the components of the inertia tensor of the space debris object, μ is the gravitational constant of the Earth, P_x, P_y are the components of the thrust force generated by the propulsion system of the active spacecraft, F_{Ix}, F_{Iy} are the components of the resultant ion force of the impulse transfer thrusters array, L_z is the resultant ion torque. The following equation is used to control the relative position of the active spacecraft.

$$P_x = k_x(x_A - x) - k_{dx}\dot{x}, \quad (6)$$

$$P_y = P_{y0} + k_y(y_A - y) - k_{dy}\dot{y}, \quad (7)$$

where x_A, y_A are the coordinates of the required relative position of the active spacecraft, k_j are control coefficients, is P_{y0} the thrust required to compensate for impulse transfer thruster.

2.2. Calculation of resultant ion force and torque for multi-beam shepherd spacecraft

To calculate the forces and torque generated by the ion beam, we use the calculation procedure described in detail in [33] and implemented by the authors in Matlab. The surface of the body is divided into triangles, after which the impact of the ion beam on each triangle is calculated. The flow parameters in the vicinity of the triangle are determined using the self-similar model of ion propagation. Assuming that, due to the low density, the particles of the intersecting ion beams do not influence each other, the total influence of N beams can be found as a geometric sum

$$\mathbf{F}_I = \sum_{j=1}^N \mathbf{F}_{Ij}(x, y, \theta, x_{Tj}, y_{Tj}, \beta_j), \quad \mathbf{L}_I = \sum_{j=1}^N \mathbf{L}_{Ij}(x, y, \theta, x_{Tj}, y_{Tj}, \beta_j) \quad (8)$$

where \mathbf{F}_{Ij} is vector of the force generated by the ion beam of the j -th impulse transfer thruster, \mathbf{L}_{Ij} is vector of ion torque generated by j -th thruster, x_{Tj} and y_{Tj} are the coordinates of the source of the j -th ion beam (P_j point on Fig. 3), β_j is the angle of the ion beam axis deviation from P_jB line connecting the center of mass of space debris and the j -th thruster (Fig. 3). The projections of the ion force on the axes of the orbital reference frame $Bx_o y_o$ can be found as

$$F_{Ix} = \sum_{j=1}^N (F_{Ijx} \cos \gamma_j + F_{Ijy} \sin \gamma_j), \quad F_{Iy} = \sum_{j=1}^N (F_{Ijy} \cos \gamma_j - F_{Ijx} \sin \gamma_j) \quad (9)$$

where $\cos \gamma_j = \frac{y_{Ti}}{\sqrt{x_{Ti}^2 + y_{Ti}^2}}$, $\sin \gamma_j = \frac{x_{Ti}}{\sqrt{x_{Ti}^2 + y_{Ti}^2}}$, F_{Ijx} and F_{Ijy} are calculated for single j -th impulse transfer thruster case when active spacecraft position is $x=0$, $y = \sqrt{x_{Tj}^2 + y_{Tj}^2}$ (Fig. 3b).

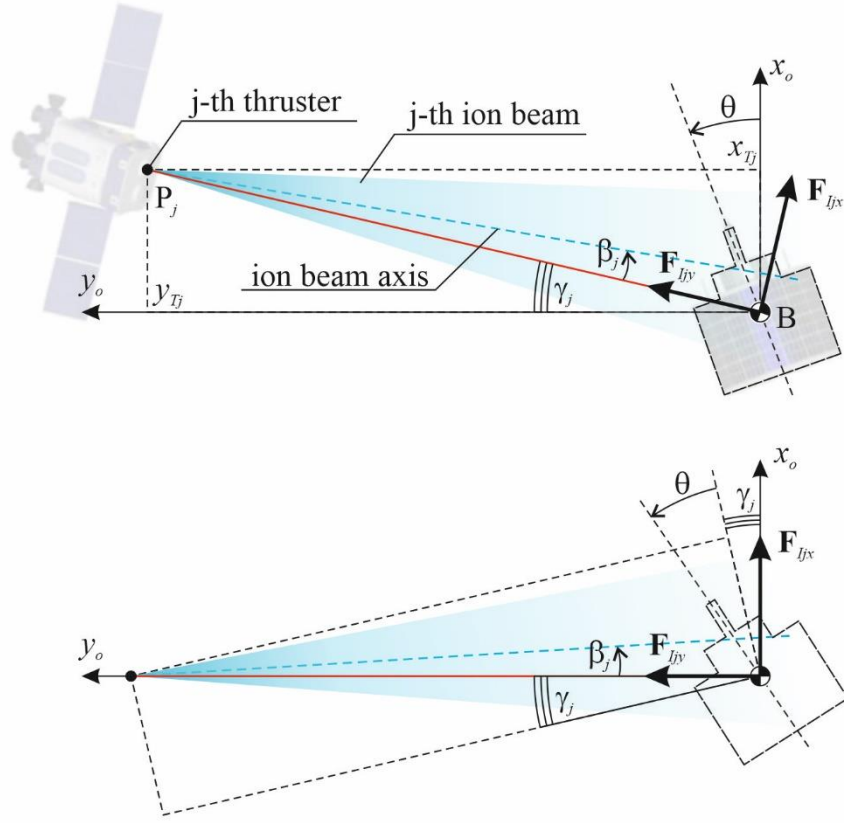


Fig. 3. Ion force components for j -th impulse transfer thruster.

To calculate the ion force generated of the j -th thruster \mathbf{F}_{ij} using the calculation procedure [33] it is required to know some ion beam parameters, in particular: the plasma density at the beginning of the far region of the ion beam n_0 , the ion velocity axial component u_0 , the ion beam divergence angle α_0 , the mass of the ion m_i , and the radius of the beam at the beginning of the far region R_0 . In scientific papers devoted to electric propulsion systems, these parameters are usually not given. Most often in such articles we can find total thruster input power P_{in} , total specific impulse I_{sp} , thrust F_T , and total efficiency η . Let's write down the expressions connecting the engine parameters with the parameters required for the calculation procedure. The ion velocity axial component can be approximately considered equal to the effective exhaust velocity of the thruster, which is

$$u_0 = V_{eff} = g_0 I_{sp}, \quad (10)$$

where $g_0 = 9.80665 \text{ m/s}^2$ is the Earth gravitational acceleration at sea level. The radius of the thruster nozzle can be used as the radius R_0 . The plasma density at the beginning of the far region for a thruster with a round nozzle can be approximately calculated as

$$n_0 = \frac{\dot{m}^2}{m_i \pi R_0^2 F_T}, \quad (11)$$

where \dot{m} is mass flow rate, which can be calculated as

$$\dot{m} = \frac{F_T}{I_{sp} g_0}, \quad (12)$$

or found from the expression for the total efficiency

$$\eta = \frac{F_T^2}{2\dot{m}P_{in}}. \quad (13)$$

Similar to the calculation of aerodynamic forces and torques, the calculation of ion forces and torques generated by an ion beam depends on the shape of the object placed in the ion beam and its orientation in the beam. Since the ion beam propagates in a rather narrow cone, the ion force and torque depend not only on the body orientation, but also on its position inside this cone, since, unlike aerodynamic forces, the parameters of the particle flow in its different parts are different. In addition, a part of the body may be outside of this cone. These circumstances make it much more difficult to model the motion of a body taking into account the impact of the ion beam. It is required either to perform a resource-intensive calculation of the ion force and torque at each integration step, or to approximate data from a pre-calculated database to obtain the force and torque values depending on the current position and orientation of the body. The latter approach is used, for example, in studies [22,31].

2.3. Ion multi-beam control schemes

Previous studies have shown that to control the angular motion of space debris, the most preferred method of control is to change the direction of the ion beam axis [21]. The controlled deflection of the beam allows the generation of an

ion torque, which tends to turn the object in the desired direction. With regard to an active spacecraft equipped with several impulse transfer thrusters, several control schemes can be proposed:

- 1) relay control based on turning on and off one of the thrusters;
- 2) changing the axis direction of one of the thrusters while maintaining the direction of the axes of other thrusters.

Regardless of which scheme is used, eventually the system is transferred to one of two states, which are characterized by the sign of the generated resultant ion torque over the entire range of angle θ (Fig. 4). After transferring the transported object to the required angular motion mode, the active spacecraft goes into the transportation mode, which implies the use of all impulse transfer thrusters.

To control an active spacecraft and switch between the states described above, it is proposed to use a control law based on an estimate of the energy of unperturbed motion. Such approach was used to control the direction of the axis of the ion beam of one thruster in the study [31]. Unperturbed motion is understood as the motion of a space debris object in a circular orbit under the action of an ion beam, when the active spacecraft occupies a constant relative position. In this case, equation (3) takes the form

$$\ddot{\theta} = \frac{L_z(\theta, s)}{I_z} + \frac{3\mu(I_x - I_y)\sin\theta\cos\theta}{I_z r^3}, \quad (14)$$

where s is the parameter that determines the state of the active spacecraft. The value $s = 0$ corresponds to the transportation mode, $s = 1$ corresponds to the case $L_z > 0$, and $s = 2$ corresponds to the case $L_z < 0$ (Fig. 4).

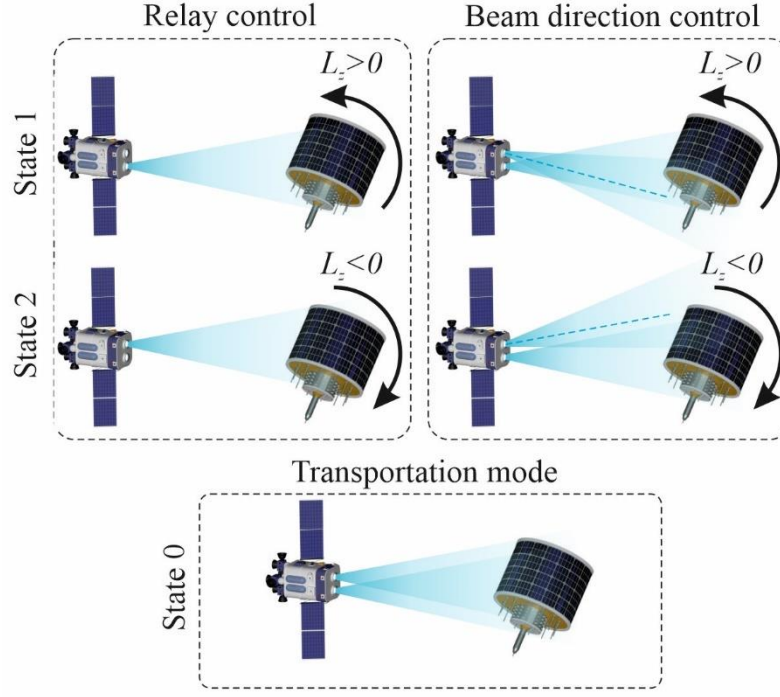


Fig. 4. Ion force components for j -th impulse transfer thruster.

For equation (14), the energy integral can be calculated as

$$E(\theta, \dot{\theta}, s) = \frac{\dot{\theta}^2}{2} - \frac{\int L_z(\theta, s) d\theta}{I_z} - \frac{3\mu(I_y - I_x) \cos 2\theta}{4I_z r^3}. \quad (15)$$

The considered unperturbed system is conservative and the energy E retains its value along each phase trajectory. If the phase portrait of the unperturbed system contains a separatrix that divides the phase plane into several oscillation regions, then one energy value can correspond to several phase trajectories located in different oscillation regions. In this case, the energy value E_* and the boundaries of the oscillation regions θ_1, θ_2 must be specified to identify the phase trajectory. Due to the conservatism of the unperturbed system $E(\theta_1, 0, 0) = E(\theta_2, 0, 0)$. In the absence of equilibrium positions, the energy uniquely determines the trajectory. The condition for the absence of an equilibrium position for equation (14) can be written as

$$|L_z(\theta, s)| > \frac{3\mu |I_x - I_y|}{2r^3} = L_{zmin}. \quad (16)$$

In the case when the perturbed motion of the system is considered, the orbit semi-latus rectum p can be taken instead of the radius r when calculating the energy (15) and limit value L_{zmin} in condition (16). For a mission of space debris removal in low Earth orbit, it is reasonable to take the radius of the atmosphere boundary as the radius r in condition (16). In this case, the condition $|L_z(\theta, s)| > L_{zmin}$ will also hold for higher orbits.

Consider the issue of transferring the system to an angular motion mode characterized by the energy $E_* = E(\theta_*, \dot{\theta}_*, 0)$, calculated by the equation (15), where $\dot{\theta}_*(\theta_*)$ is the required phase trajectory. The phase trajectory intersects the axis $\dot{\theta} = 0$ at the points θ_{*1} and θ_{*2} . If the target trajectory is the equilibrium position, then $\theta_{*1} = \theta_{*2} = \theta_*$. It is assumed that for State 1 ($s = 1$) and State 2 ($s = 2$) condition (16) is satisfied. In this case, the phase portrait and the dependence of the energy on the angle θ for States 1 and 2 are schematically shown in Fig. 5. To transfer the representative point of the system from an arbitrary state to the target trajectory, it is proposed to switch the state of the system in accordance with Table 1. In order to switch from one state to another in time, at each integration step, one should track the energies corresponding to states different from the current state and compare them with the conditions in Table 1.

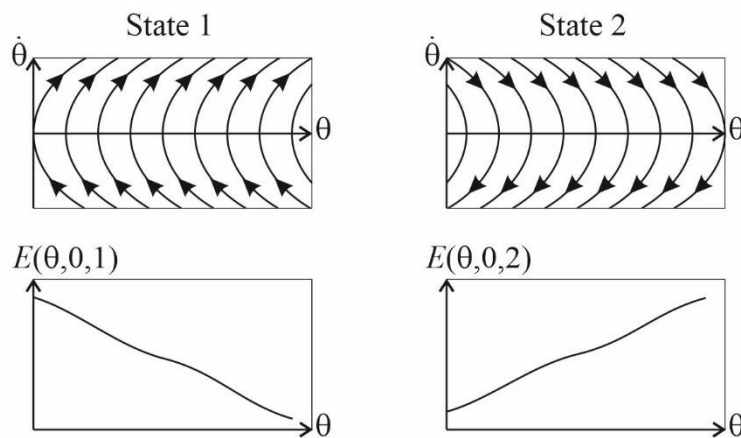


Fig. 5. Schematic representation of the phase portrait and energy for the case of controlled motion of space debris in States 1 and 2

Table 1. Control strategy

| Current angular velocity , $\dot{\theta}$ | Current energy, E | Control state, s (Fig. 4) |
|---|--|-----------------------------|
| $\dot{\theta} \leq 0$ | $E(\theta, \dot{\theta}, 1) < E(\theta_{*2}, 0, 1)$ | 2 |
| $\dot{\theta} \leq 0$ | $E(\theta, \dot{\theta}, 1) \geq E(\theta_{*2}, 0, 1)$ | 1 |
| $\dot{\theta} > 0$ | $E(\theta, \dot{\theta}, 2) < E(\theta_{*1}, 0, 2)$ | 1 |
| $\dot{\theta} > 0$ | $E(\theta, \dot{\theta}, 2) \geq E(\theta_{*1}, 0, 2)$ | 2 |
| $\dot{\theta} \in (-\infty, \infty)$ | $E(\theta, \dot{\theta}, 0) = E(\theta_{*1}, 0, 0)$ | 0 |
| Other cases | | 0 |

Fig. 6 schematically shows the translation of the imaging point in the phase space $(\theta, \dot{\theta})$ to the target trajectory using the described above approach. The yellow color shows the area where, according to Table 1, the spacecraft must be transferred to State 1. The area marked in blue is where the state should be set to State 2. Bold black lines on the boundary of the regions show the phase trajectories having energy $E(\theta_{*2}, 0, 1)$ and $E(\theta_{*1}, 0, 2)$ in States 1 and 2, respectively. The point A at the initial moment of time has an angular velocity $\dot{\theta} < 0$ and an energy $E(\theta, \dot{\theta}, 1) \geq E(\theta_{*2}, 0, 1)$. In this case, the conditions of the second row of Table 1 are met. After the trajectory passes the abscissa axis (point B), it enters the area $\dot{\theta} > 0$, where $E(\theta, \dot{\theta}, 2) < E(\theta_{*1}, 0, 2)$, and the conditions in the third row of Table 1 are met. At point C, the energy reaches the value $E(\theta, \dot{\theta}, 2) = E(\theta_{*1}, 0, 2)$, which means that the conditions of the fourth row from the table are satisfied. At this point, the system switches to State 2. Further motion occurs up to point θ_{*1} of the target trajectory, where $E(\theta, \dot{\theta}, 0) = E(\theta_{*1}, 0, 0) = E(\theta_{*2}, 0, 0)$ and the spacecraft is transferred to State 0. It should be noted that if the imaging point at the initial moment of time is inside the area limited by the target phase trajectory, then the transition to this trajectory can be carried out both by transferring the active spacecraft to State 1 and State 2.

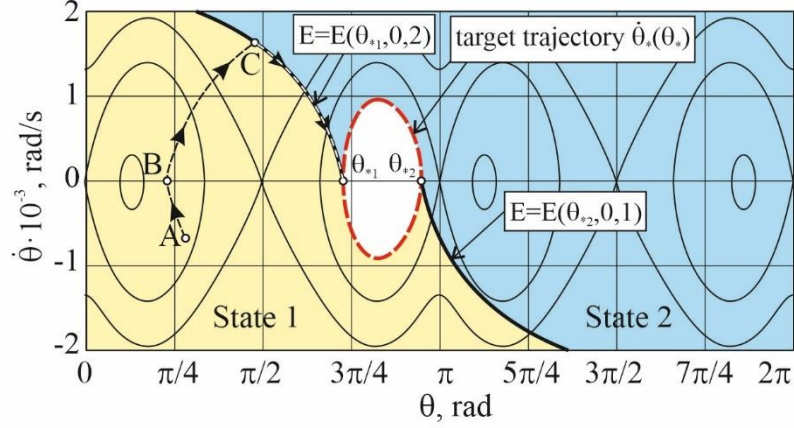


Fig. 6. Phase portrait for State 0 and various control areas

3. Numerical simulations

3.1. Fuel consumption for various thrusters' layouts

To evaluate the efficiency of using several ion beams to solve the problem of active space debris removal, let us simulate the space debris contactless transportation without controlling its attitude motion. In this subsection it is assumed that during the entire transportation, the axis of all impulse transfer thrusters passes through the center of mass of the space debris object. The control system of the active spacecraft keeps it in the relative position $x=0$, $y=15\text{m}$, so the distance between the transportation system and the space debris is 15m. The plane on which the impulse transfer thrusters' nozzles are located is perpendicular to the line AB connecting the centers of mass of the active spacecraft and the space debris object (Fig. 2).

Various cases are discussed below when the active spacecraft is equipped with one, two or three thrusters. The layout of engine nozzles on the surface of an active spacecraft is shown in Fig. 7. The displacement of the axis of the first and third engines from the axis is $h=0.5\text{m}$. The third column in Table 2 indicates which position of the thrusters corresponds to each of the considered cases. In our calculations, we will be guided by the NASA Evolutionary Xenon Thruster Commercial (NEXT-C) gridded ion thruster [34], the parameters of which are given

in Table 3. The ion beam parameters calculated using formulas(10)-(12), which are necessary for obtaining the ion forces and torque, are given in Table 4. In this study, the ion beam divergence angle is taken as 10 deg , since the authors could not find this parameter in the sources. Article [35] describes laboratory studies of the simultaneous operation of three NEXT thrusters. Research results show that the use of an array of thrusters does not lead to a decrease in the performance of each of them. Since the development of technology allows us to hope for the creation of more efficient engines, in addition to cases involving the use of one and several NEXT-like engines (cases 1-4), we will also consider cases of using a hypothetical engine that generates thrust equal to two and three NEXT engines (cases 5, 6). It is assumed that other parameters of the hypothetical thruster (nozzle radius, specific impulse) are the same as those of the array thruster.

Table 2. Compared cases

| Case | Number of thrusters | Thrusters' locations (Fig. 7) | Total thrust, mN | Required Power kW | Mass of fuel consumed, kg | Mission time, hours |
|------|---------------------|-------------------------------|------------------|-------------------|---------------------------|---------------------|
| 1 | 1 | 2 | 235 | 7.33 | 85.68 | 1949.5 |
| 2 | 2 | 1,2 | 470 | 14.66 | 86.08 | 978.9 |
| 3 | 2 | 1, 3 | 470 | 14.66 | 86.01 | 978.8 |
| 4 | 3 | 1,2,3 | 705 | 21.99 | 86.14 | 653.6 |
| 5 | 1 | 2 | 470 | 14.66 | 85.90 | 977.6 |
| 6 | 1 | 3 | 705 | 21.99 | 86.02 | 652.7 |

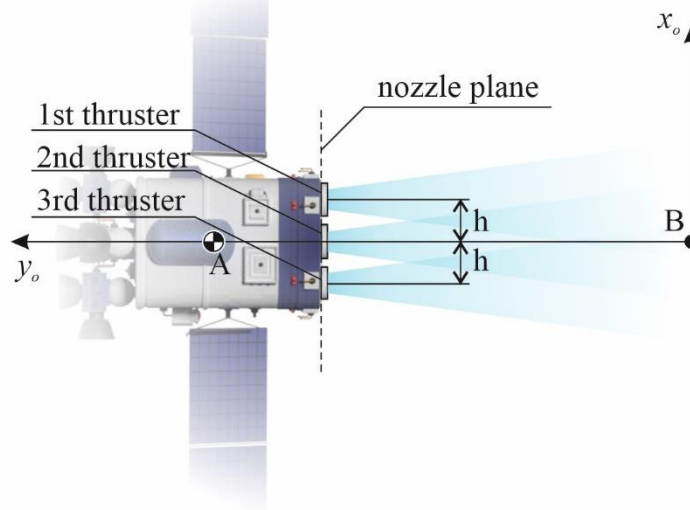


Fig. 7. Impulse transfer thrusters' location

Table 3 - NEXT-C parameters

| Parameter | Values |
|--------------------------------------|---------|
| Input power P_{in} | 7.33 kW |
| Thruster efficiency η | 0.7 |
| Thrust F_T | 235 mN |
| Specific impulse I_{sp} | 4155 s |
| Nozzle radius R_0 | 0.18 m |
| Ion thruster mass m_{IT} | 14 kg |
| Power processing unit mass m_{PPU} | 36 kg |

Table 4 - Ion beam parameters

| Parameter | Values |
|--------------------------------|---------------------------------------|
| Velocity axial component u_0 | 40747 m/s |
| Plasma density n_0 | $6.3787 \cdot 10^{15} \text{ m}^{-3}$ |
| Mass flow rate \dot{m} | $5.7673 \cdot 10^{-6} \text{ kg/s}$ |

| | |
|-----------------------------|---------------------------------|
| Xenon ion mass m_i | $2.18 \cdot 10^{-25} \text{kg}$ |
| Divergence angle α_0 | 10deg |

As an example, let us consider the removal of the Vostok second stage (SL-3), which mass is 1440 kg, length is 3.8 m, radius is 1.3 m [36]. It is assumed that the stage is a cylinder, the center of mass of which is located in its geometric center. The moments of inertia are calculated for an ideal cylinder case. The longitudinal moment of inertia is $2434 \text{ kg} \cdot \text{m}^2$, and the transverse moment of inertia is $1733 \text{ kg} \cdot \text{m}^2$. The stage moves in an elliptical orbit with an apoapsis height of 737 km and a periapsis height of 666.4 km. Figs. 8-10 show the dependences of the projections of the resultant ion force and torque on the axis of the orbital coordinate system, calculated for various ways of placing the thrusters given in Table 2. The shift of curve 2 in Fig. 8 to the negative area from other curves is due to the asymmetry of the thrusters' location in Case 2. As can be seen from Figs. 9 and 10, an increase in the total thrust of the engine array leads to an increase in the magnitude of the generated ion force and torque. In this case, the points of intersection of the curves L_z with the abscissa axis, which in the absence of a gravity gradient torque are the positions of equilibrium for the angle θ , remain unchanged in Cases 1, 3-6 and displaced very slightly in Case 2.

Let us simulate the descent of the stage until the moment when the periapsis height of its orbit drops to an altitude of 100 km using equations (1)-(5). In all cases it is assumed that the initial mass of the spacecraft is $m_{A0} = 700 \text{kg}$, of which $m_{f0} = 200 \text{kg}$ is the fuel reserve. The following initial conditions are used in the simulation

$$r_0 = 7037400 \text{m}, \dot{r}_0 = 0, \nu_0 = 0, \dot{\nu} = 1.0668 \cdot 10^{-3} \text{ rad/s}, \theta_0 = 3.84 \text{rad}, \dot{\theta}_0 = 0, x_0 = 0, \\ \dot{x}_0 = \dot{y}_0 = 0, y_0 = 15 \text{m}.$$

The diameter of the ion beam at the center of mass of the stage in the case of one thruster is 5.29m. The ratio of the beam diameter to the stage length is 1.39. The following values are taken as parameters of control laws (6)-(7)

$$k_x = k_y = 1000 \text{ kg/s}^2, k_{dx} = k_{dy} = 1000 \text{ kg/s}, P_{y0} = -0.247 F_T \frac{m_A}{m_B}$$

where F_T is the thrusters' array total thrust given in fourth column of Table 2. The use of control laws (6)-(7) requires tracking the relative position and relative velocity of the active spacecraft. To simulate the change in mass of the active spacecraft $m_A = m_{A0} - m_f$, the following differential equation is used

$$\dot{m}_f = \frac{2NF_T}{I_{sp}g_0} + \frac{|P_x| + |P_y|}{I_{sp}g_0}, \quad (17)$$

where m_f is mass of the fuel consumed. The factor 2 in the first term of equation (17) is due to the need to compensate for thrust of the spacecraft's impulse transfer thrusters by an additional compensation thrusters. For simplicity, it is assumed that the specific impulses of all spacecraft's thrusters are the same.

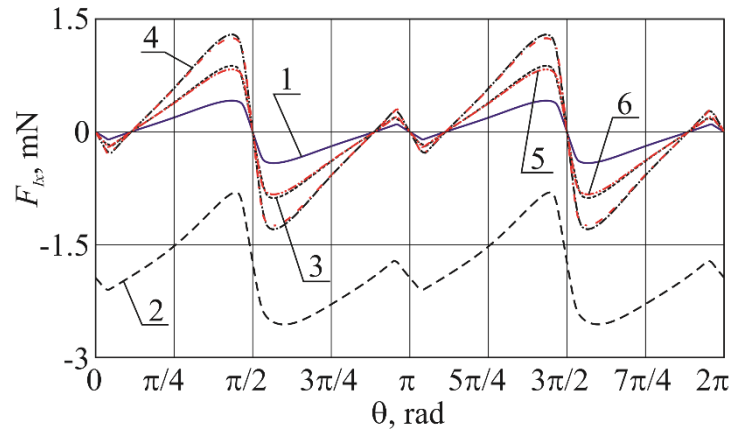


Fig. 8. Dependence of ion force projection F_{lx} on the deflection angle θ

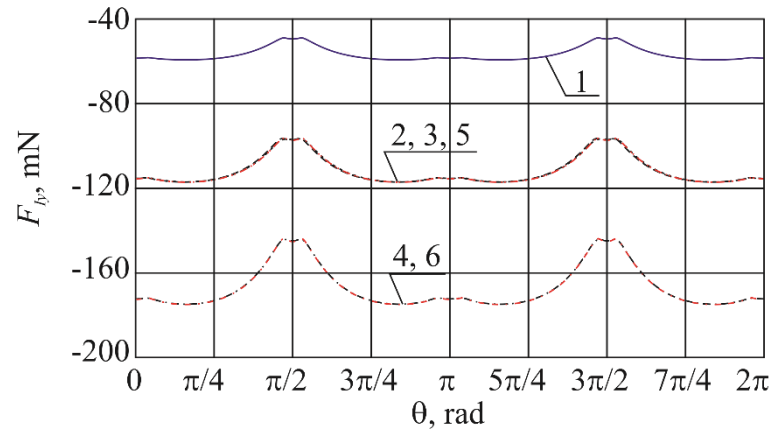


Fig. 9. Dependence of ion force projection F_y on the deflection angle θ

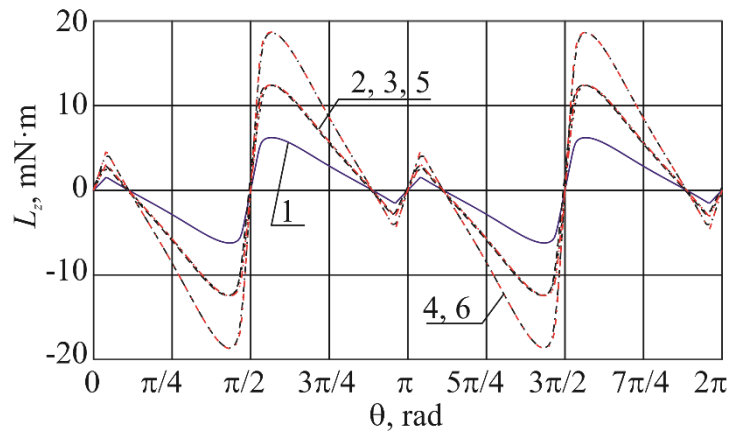


Fig. 10. Dependence of ion torque projection L_z on the deflection angle θ

Calculations show that in all simulated cases, the space debris object oscillates around the equilibrium position throughout the entire descent. The two right columns of Table 2 show the mass of fuel and the time of descent. A multiple increase in thrust leads to a significant decrease in the descent time. Despite the fact that the operating time of the thrusters is reduced, the installation of an additional thrusters increases fuel consumption per unit of time. As cases 2-4 show (Table 2), adding a thruster leads to an increase in the mass of fuel consumed compared to case 1, which implies the use of a single thruster. Comparing cases 2 and 3, it can be concluded that the asymmetrical placement of the thrusters does not lead to a significant change in the mass of the required fuel. It should be noted that in all cases, changes in mass are insignificant and do not exceed 0.46 kg.

3.2. Choice of angles of inclination of the ion beam axes

To investigate the influence of the angle of ion beam axis deviation on the magnitude of the generated ion force, let us perform a series of numerical calculations. It is assumed that the active spacecraft is equipped with two thrusters located symmetrically in accordance with Case 3 from Table 2. We restrict ourselves to the study of the case when the axes of the thrusters are rotated symmetrically by the angles β and $-\beta$, respectively. Fig. 11 shows the dependence of the projection of the ion force F_{ly} for various values of the angle β . The maximum value of ion force corresponds to the angle $\beta = -1.9^\circ$ when the ion beam axes pass through the geometric center of the cylinder. Fig. 12 demonstrates a bifurcation diagram showing the change in the equilibrium positions of the angle θ with a change in the angle β . This diagram is built using equation (14) for the case of a circular orbit. The phase portrait for the case $\beta = -1.9^\circ$ and a height of the circular orbit of 500 km is shown in Fig. 13. Center-type equilibrium positions correspond to a black solid line on the bifurcation diagram (Fig. 12), and unstable saddle points correspond to a red dashed line.

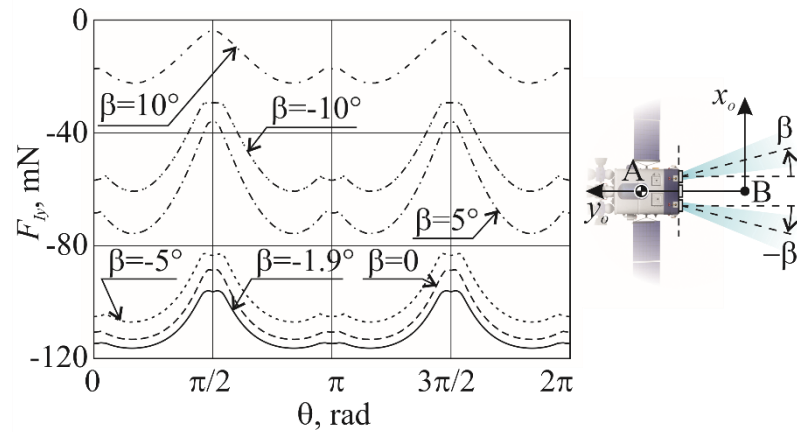


Fig. 11. Dependence of ion force projection F_{ly} on the deflection angle θ

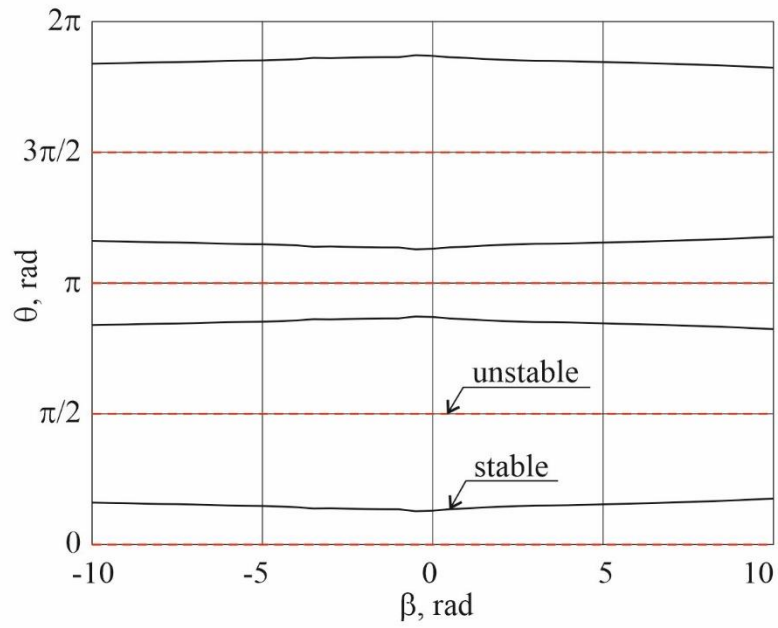


Fig. 12. Bifurcation diagram

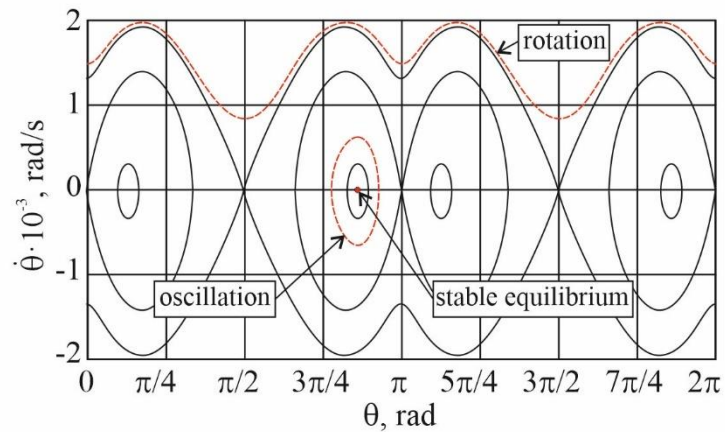


Fig. 13. The dependence of the mass of spent fuel on time

3.3. Choice of the most preferred angular motion mode of space debris

According to the phase portrait shown in Fig. 13, in the case of unperturbed motion corresponding to motion in a circular orbit under the action of an ion beam, a space debris object can perform angular motion related to one of three types: be in a position of stable equilibrium, oscillate or rotate. In the last two cases, the angle of the object deflection θ from the local vertical is constantly changing, which leads to a change in the force generated by the ion beam. The average ion force \bar{F}_y calculated on the period of the object's oscillations T can be used as a measure of

the effectiveness of the angular motion mode for the considered mission of contactless transportation

$$\bar{F}_{ly} = \frac{1}{T} \int_0^T F_{ly}(\theta(t)) dt. \quad (18)$$

Fig. 14 shows a graph of the average force dependence on angle θ_0 . For each value of θ_0 , a numerical calculation was carried out. Equation (14) was integrated for the initial conditions $\theta(0) = \theta_0$, $\dot{\theta}(0) = 0$ and then the average force was calculated using (18). Case 3 (Table 2), when two engines are used and the ion beam axes pass through the geometric center of the object, was used for the calculation.

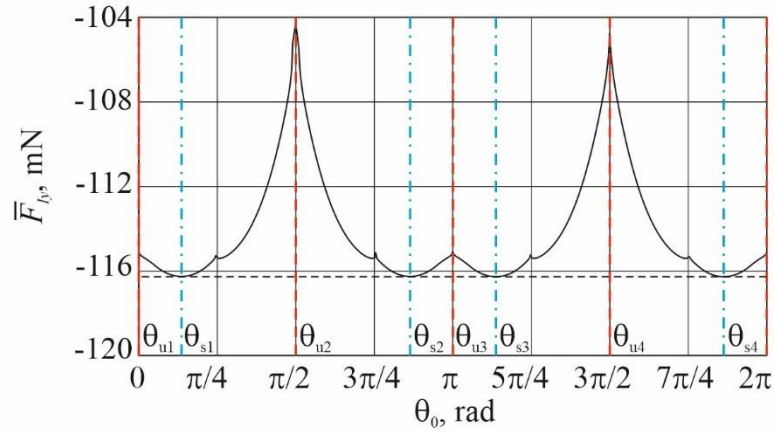


Fig. 14. The dependence of the average ion force projection on the space debris object deflection angle θ_0

Calculations show that for the considered case, the most favorable is transportation in a stable equilibrium position θ_{sj} . These positions are shown in Fig. 14 by blue dash-dotted lines. The maximum magnitude of the force is $\bar{F}_{ly \max} = |\min_{\theta_0 \in [0, 2\pi]} \bar{F}_{ly}(\theta_0)| = 0.1163 \text{ N}$. The minimum magnitude of the average force $\bar{F}_{ly \min} = |\max_{\theta_0 \in [0, 2\pi]} \bar{F}_{ly}(\theta_0)| = 0.1043 \text{ N}$ is observed in unstable positions θ_{s2} and θ_{s4} , when the object is oriented with a flat end surface to the flow. The values of the average force at the points of local minima and maxima coincide due to the symmetry of the ion beams and the considered space debris object. Fig. 15 shows the dependence of the average ion force on the initial angular velocity, for the case

of rotation. Integration was carried out under initial conditions $\theta(0) = \pi / 2$, $\dot{\theta}(0) = \dot{\theta}_0$. As the angular velocity increases, the averaged ion force tends to the value $\bar{F}_{ly} = -0.111\text{N}$.

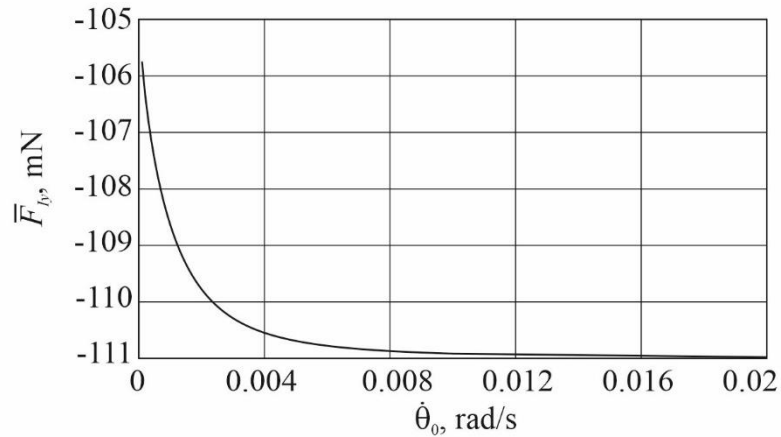


Fig. 15. The dependence of the average ion force projection on the space debris angular velocity $\dot{\theta}_0$

Comparing Figs. 14 and 15, it can be concluded that transportation in the oscillation mode and in the position of a stable equilibrium is more efficient in terms of the magnitude of the generated ion force than in the rotation mode. Numerical simulations of the most favorable and unfavorable regimes using equations (1)-(5), when the space debris object is in equilibrium positions $\theta_0 = 3.5655\text{rad}$ and $\theta_0 = \pi / 2$, respectively, show that in the favorable case, the mission lasts 974.0 hours and requires 85.61 kg of fuel, and in the unfavorable case, the required time and fuel consumption increase to 1055.1 hours and 92.35 kg. Taking the unfavorable case as 100%, when the object is transferred to a stable equilibrium position, the fuel savings are 7.3%.

3.4 Space debris attitude motion control

Consider the case when the space debris object is in an unfavorable angular regime determined by the initial conditions $\theta_0 = \pi / 2$, $\dot{\theta}_0 = 0$. The goal of control is to transfer the space debris object to position θ_{s3} (Fig. 14), corresponding to a

favorable regime. As in the previous subsection, it is assumed that the active spacecraft is equipped with two impulse transfer thrusters located in positions corresponding to Case 3 from Table 2. In accordance with the results of Section 3.2, the ion beams axes are directed towards the geometric center of the space debris object to provide the most efficient contactless transportation mode. Consider the two control schemes described in Section 2.3. Relay control of impulse transfer thrusters assumes that the axes of the ion beams cannot change their direction. Angular motion control is achieved by turning the thrusters on and off. Ion beam axis direction control assumes that one of the impulse transfer thrusters (thruster 1 in Fig. 7) is installed on a swiveling platform and can turn relative to the active spacecraft using an electric motor. The second thruster constantly maintains the direction of the axis of its beam.

To implement the control law described in Section 2.3, the ion torque in State 1 and 2 must satisfy the inequality (16). For the considered space debris, the ion torque limit value is $L_{zmin} = 0.0015 \text{ N m}$.

3.4.1. Relay control of impulse transfer thrusters

Calculations of the dependence of the ion torque on θ for the case of operation of one of the two thrusters show that in the case when the beam axis is directed to the geometric center ($\beta = -1.9^\circ$), condition (16) is not fulfilled and the control scheme described in Section 2.3 cannot be implemented. Increasing the angle β , which determines the direction of the ion beam axis, solves this problem, but increasing the angle leads to a decrease in the generated ion force (Fig. 11), which in turn reduces the efficiency of the ion transportation system and leads to an increase in time and fuel costs. When the value of the angle $\beta = -0.4^\circ$ condition (16) is fulfilled (Fig. 16). The black solid line in Fig. 16 indicates the resultant ion torque generated by the two thrusters in positions 1 and 3 (Fig. 7). The red dashed lines in Fig. 16 correspond to the ion torques generated by the thruster in position 1. The blue dash-dotted lines show ion torques of thruster in position 3.

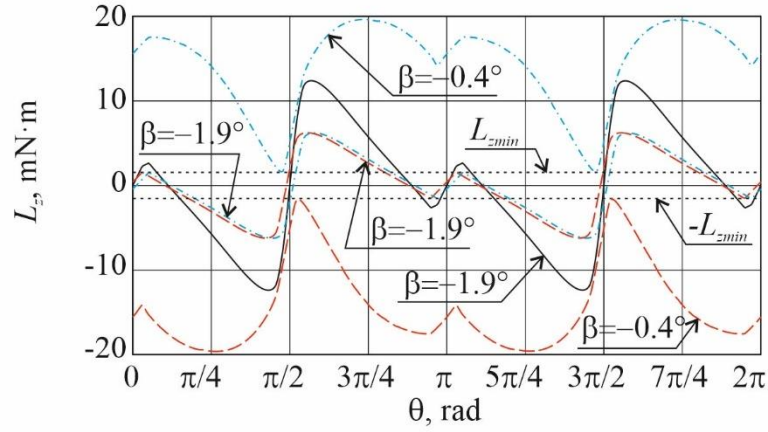


Fig. 16. Dependence of ion torque projection L_z on the deflection angle θ .

Consider a controlled descent of space debris at ion beam axis deflection angle $\beta = -0.4^\circ$. An active spacecraft can be in one of three states. In State 0, both impulse transfer thrusters are turned on. In State 1, only the thruster in position 3 is turned on, resulting in a positive ion torque. In State 2, only the thruster in position 1 is turned on, and a negative ion torque is generated. Fig. 17 demonstrates the phase trajectories for a space debris object using various control schemes. The relay control trajectory is shown by the red line. At the initial moment of time, the system is in the area where State 1 should be used. At point A_1 (Fig. 17), in accordance with the control law described in Section 2.3, the system switches to State 2. At point B_1 , the phase trajectory reaches the target equilibrium position and both engines turn on, bringing the system to State 0. Due to the fact that the considered system is not unperturbed, the representative point will not remain in the equilibrium position, but will oscillate around it with a small amplitude. Calculations show that the displacement of the representative point from the position to which the point was transferred using relay control at the initial stage of transportation does not exceed 0.035 rad (Fig. 17). The entire descent operation takes 990.3 hours and requires 86.96 kg of fuel. It should be noted that the values obtained for time and fuel turn out to be worse than those obtained in Section 3.3 for the case when the object is immediately in a favorable angular position. This deterioration is due to the fact that

angle β in this calculation has been changed, the beams axes do not pass through the center of mass of the object resulting in a decrease in ion force.

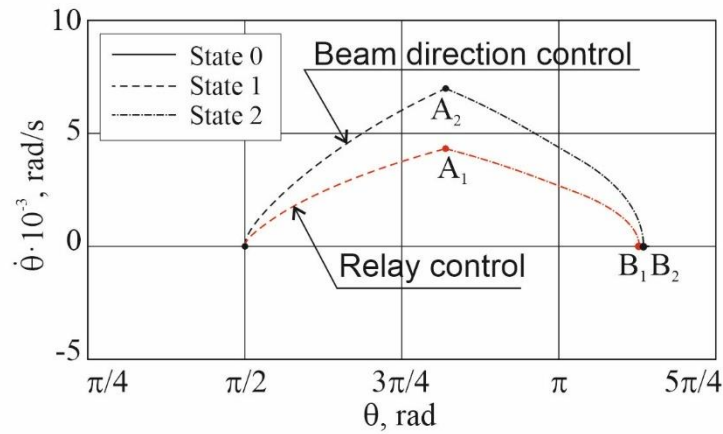


Fig. 17. Phase portraits for the case of controlled descent.

3.4.2. Ion beam axis direction control

A series of calculations using the procedure described in Section 2.2 was carried out. The goal was to determine the angles β of the first thruster's axis deflection corresponding maximum and minimum of the ion torque in States 1 and 2. Fig. 18 shows the dependences of the maximum and minimum resulting ion torque of two thrusters in positions 1 and 3 (Fig. 7) on the β angle of the first thruster. The maximum positive and minimum negative ion torque is observed at angles $\beta_1 = -8^\circ$ and $\beta_2 = 4.25^\circ$, respectively. Fig. 19 shows the corresponding dependences of the ion torques on the deflection angle of the space debris object θ .

Let's simulate a controlled descent of a space debris object using the first impulse transfer thruster to control the orientation of the object. The simulation assumes that the thruster's axis turns instantly. This is quite justified, since the period of the object's angular oscillations and the period of its orbital motion exceed 30 minutes, while the process of turning the platform with the thruster takes seconds. At the initial stage of motion, the object is in the area corresponding to State 1, so the first thrusters deviates by an angle β_1 . The phase trajectory is shown in Fig. 17 as a black line. At point A_2 , the energy $E(\theta, \dot{\theta}, 2)$ reaches the value $E(\theta_{*1}, 0, 2)$ and,

in accordance with the fourth line of Table 1, the system is switched to State 2. To do this, the first thruster rotates through an angle β_2 . At point B_2 , the phase trajectory reaches the target equilibrium position, the axis of the first engine is directed to the center of mass of the object ($\beta = -1.9^\circ$), and the system switches to State 0. Mismatch of points B_1 and B_2 in Fig. 17 is due to the mismatch of β angles in State 0 in the case of relay control and beam axis control. Calculations show that for the implementation of the transport operation for the space debris object descent from orbit, 974.1 hours and 85.61 kg of fuel are required. These values are slightly worse than those obtained in Section 3.3 when the object is immediately in a favorable angular position.

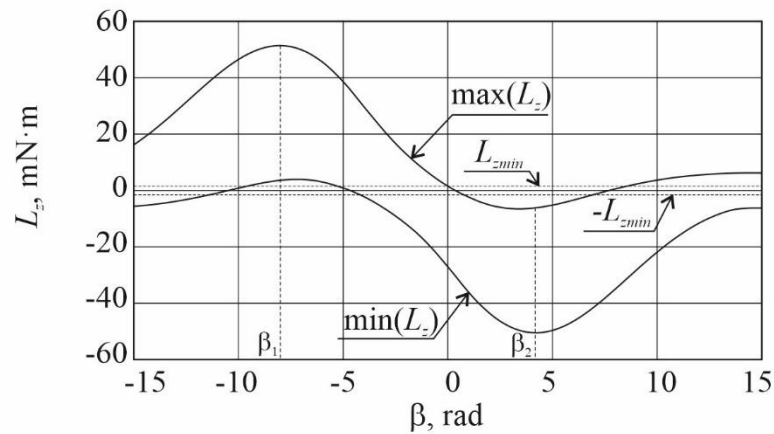


Fig. 18. Dependence of amplitude values of resulting ion torque L_z on the angle β , which determines the deviation of the axis of the ion beam of the first thruster.

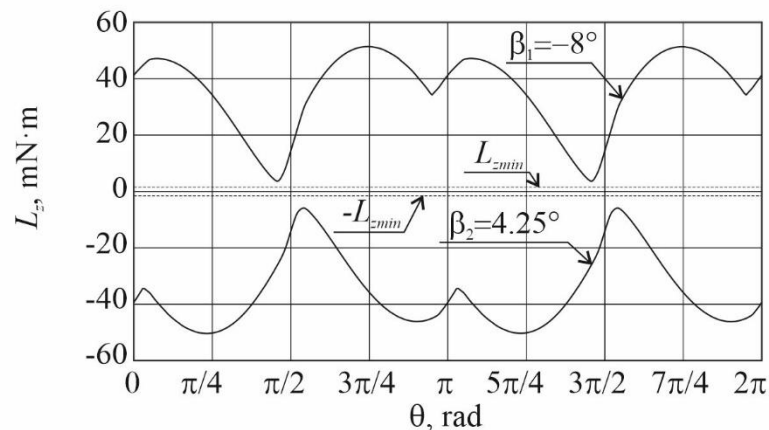


Fig. 19. Dependence of ion torque projection L_z on the deflection angle θ .

4. Discussion

As part of the study, a large number of numerical calculations were performed. The results are collected in a summary Table 5 for visual presentation. The values given in the mass column include the cost of the impulse transfer thrusters, the impulse compensation thrusters and the control engines. Obviously, using an array of impulse transfer thrusters does not result in fuel mass savings compared to using a single thruster. At the same time, an increase in the number of engines leads to a multiple decrease in the descent time, which can be of decisive importance for a space debris removal mission. Reducing the time of an object existence in orbit reduces the probability of its collision with other objects. Since the mass of required fuel does not change much when using a different number of engines, the failure of one of them does not lead to mission failure. The mission can be completed with one thruster, it just takes more time.

Table 5 – Summary of calculations results

| Case | Number of thrusters | Thrusters' locations (Fig. 7) | Total thrust, mN | Initial angle θ_0 , rad | Attitude control | Section | Mass of fuel consumed, kg | Mission time, hours |
|------|---------------------|-------------------------------|------------------|--------------------------------|------------------------|---------|---------------------------|---------------------|
| 1 | 1 | 2 | 235 | 3.84 | Uncontrolled | 3.1 | 85.68 | 1949.5 |
| 2 | 2 | 1,2 | 470 | 3.84 | Uncontrolled | 3.1 | 86.08 | 978.9 |
| 3 | 2 | 1, 3 | 470 | 3.84 | Uncontrolled | 3.1 | 86.01 | 978.8 |
| 4 | 3 | 1,2,3 | 705 | 3.84 | Uncontrolled | 3.1 | 86.14 | 653.6 |
| 5 | 1 | 2 | 470 | 3.84 | Uncontrolled | 3.1 | 85.90 | 977.6 |
| 6 | 1 | 3 | 705 | 3.84 | Uncontrolled | 3.1 | 86.02 | 652.7 |
| 7 | 2 | 1,3 | 470 | 3.5655 | Uncontrolled | 3.3 | 85.68 | 974.0 |
| 8 | 2 | 1,3 | 470 | 1.5708 | Uncontrolled | 3.3 | 92.35 | 1055.1 |
| 9 | 2 | 1,3 | 470 | 1.5708 | Relay control | 3.4.1 | 86.96 | 990.3 |
| 10 | 2 | 1,3 | 470 | 1.5708 | Beam direction control | 3.4.2 | 85.61 | 974.1 |

Calculations shown that the use of additional thrusters does not entail a significant change in the mass of fuel, however, their installation leads not only to an increase in the generated ion force, but also to an increase in the mass of the entire propulsion system of an active spacecraft. For a given mass budget, this means a reduction in the mass of propellant that a spacecraft can carry. The use of an additional engine also requires additional power consumption. This can also lead to an increase in spacecraft's dry mass due to the installation of additional segments of solar panels and batteries (Fig. 1). An increase in the active spacecraft size due to the installation of additional solar arrays will increase the likelihood of its collision with other space debris during transportation. In this study it was assumed that the system is in "clean" space and there is no need to perform collision avoidance maneuvers. Trajectory planning taking into account the orbital motion of other objects will increase the time and cost of the removal operation. These circumstances should be analyzed in detail when developing the design of the active spacecraft and preparing a multipurpose mission of active space debris removal.

Calculations show that the development and use of a more advanced impulse engine that generates more thrust while maintaining the specific impulse does not lead to a qualitative improvement in the required time and fuel mass compared to using an array of thrusters. One of the possible advantages of using a single thruster compared to an array is the absence of efficiency losses in the force generated on the surface of the transported object as a result of the interaction of particles in the beams of different thrusters. In carrying out this study, the mutual influence of intersecting ion beams on each other was not taken into account. This issue requires careful study, requiring laboratory experiments and detailed modeling of the interaction of thrusters' plumes. As a result of such studies, loss factors can be determined, which should be used in calculating the generated ion force and torque.

The results obtained in Section 3 apply only to the Vostok second stage in the case when the center of mass coincides with its geometric center. For objects of other geometry and layout, ion force and torque must be recalculated. A change in these force and torque will entail a change in the equilibrium positions and the location of

the most favorable and unfavorable modes of the object's angular motion for contactless transportation. The boundary value of the ion torque (16), which determines the possibility of using the method of controlling the angular position of an object described in Section 2.3, will also change.

The results of numerical simulation showed that the control law for the angular position of a transported object, proposed in Section 2.3, based on calculating the energy in the unperturbed case of a circular orbit, also works well for orbits with a small eccentricity. The possibility of using this scheme for orbits with a large eccentricity requires additional research, which involves identifying the limits of applicability of the control law and its possible modification.

The article considers two ways to control the transported object angular motion: relay control, which involves turning the thrusters on and off, and controlling the direction of the beam of one of the thrusters. The first method is simpler in terms of technical implementation, since it does not require modification of the active spacecraft design. The second method showed the best efficiency, but its implementation requires the installation of a thruster on a rotating platform, which is controlled by an electric motor. The transient time, over which the object is transferred from the initial to the target angular position, in the first and second schemes is 1051 s and 659 s, respectively. The lower efficiency of the first method is due to the need to increase the angle β to fulfill condition (16). As a result, after the system is transferred to the equilibrium position, the generated ion force turns out to be less than in the case where the beams axes pass through the object's center of mass. An alternative to increasing the β angle could be to move the active spacecraft along the By_o axis closer or farther to the space debris object while maintaining the direction of the ion beam axes. However, when the distance between the active spacecraft and the object changes, the equilibrium positions also change, which makes it impossible to use the proposed control law and requires its significant modification. Section 3.4 investigates the case when the active spacecraft is equipped with two impulse transfer thrusters. The use of more thrusters may require modification of the control scheme, determination of an effective way of

positioning and orienting the thrusters, taking into account the characteristics of the transported object.

5. Conclusion

The paper proposes a modification of the ion beam shepherd concept by using array of thrusters. Using several ion beams allows to increase generated resultant ion beam force. A plane case of motion of a mechanical system consisting of an active spacecraft and a cylindrical space debris object is considered. A control law for the impulse transfer thrusters of an active spacecraft based on the calculation of the energy of a space debris object unperturbed oscillations is proposed. The control law ensures the transfer of the space debris object to the required angular mode of motion. Two control schemes are proposed that use the developed control law: relay control based on turning on and off one of the thrusters; and ion beam axis direction control of one of the thrusters while maintaining the direction of the axes of other thrusters. An analytical condition for the ion torque, which must be satisfied in order to be able to implement the developed control law, is obtained. A numerical study of the removal of cylindrical space debris from low Earth orbit for a different number and location of ion thrusters is carried out. For the case of two symmetrically located thrusters, the influence of the angle of deviation of the ion beam axis from the line connecting the centers of mass of the active spacecraft and space debris on the value of the generated ion force is studied. The most favorable and unfavorable angular motion modes of space debris object are revealed. Numerical simulation of the system's controlled motion, which ensures the transfer of a space debris object from an unfavorable to a favorable angular motion mode, is carried out using proposed control schemes and law. Calculations have shown that the control scheme based on changing the direction of the ion beam of one of the thrusters is more efficient than relay control scheme. The transition process takes less time, and the entire space debris removal mission requires less fuel and time. For the considered case, the fuel savings in the case of relay control and beam direction control compared to

uncontrolled descent in an unfavorable angular mode are 5.8% and 7.3% respectively.

The use of an array of impulse transfer thrusters improves the environmental safety of the system, since it reduces the time required to complete the space debris removal mission, and also increases the reliability of the system, since the failure of one of the thrusters does not lead to mission failure. Controlling the angular motion of a space debris object makes it possible to reduce time and fuel costs. The use of multiple ion beams can be effective for contactless transportation of large objects of complex shape. It opens up new possibilities for creating new ion beam shepherd spacecraft design and developing new control methods and laws.

Acknowledgments

This study was supported by the Russian Science Foundation (Project No.22-19-00160).

References

- [1] H.G. Lewis, Understanding long-term orbital debris population dynamics, *J. Sp. Saf. Eng.* 7 (2020) 164–170. <https://doi.org/10.1016/j.jsse.2020.06.006>.
- [2] J.-C. Liou, N.L. Johnson, N.M. Hill, Controlling the growth of future LEO debris populations with active debris removal, *Acta Astronaut.* 66 (2010) 648–653. <https://doi.org/10.1016/j.actaastro.2009.08.005>.
- [3] C. Bonnal, J.M. Ruault, M.C. Desjean, Active debris removal: Recent progress and current trends, *Acta Astronaut.* 85 (2013) 51–60. <https://doi.org/10.1016/j.actaastro.2012.11.009>.
- [4] A. Rossi, A. Petit, D. McKnight, Short-term space safety analysis of LEO constellations and clusters, *Acta Astronaut.* 175 (2020) 476–483. <https://doi.org/10.1016/j.actaastro.2020.06.016>.
- [5] D. McKnight, R. Witner, F. Letizia, S. Lemmens, L. Anselmo, C. Pardini, A. Rossi, C. Kunstadter, S. Kawamoto, V. Aslanov, J.-C. Dolado Perez, V. Ruch, H. Lewis, M. Nicolls, L. Jing, S. Dan, W. Dongfang, A. Baranov, D.

- Grishko, Identifying the 50 statistically-most-concerning derelict objects in LEO, *Acta Astronaut.* 181 (2021) 282–291.
<https://doi.org/10.1016/j.actaastro.2021.01.021>.
- [6] H. Hakima, M.R. Emami, Assessment of active methods for removal of LEO debris, *Acta Astronaut.* 144 (2018) 225–243.
<https://doi.org/10.1016/j.actaastro.2017.12.036>.
- [7] C.P. Mark, S. Kamath, Review of Active Space Debris Removal Methods, *Space Policy.* 47 (2019) 194–206.
<https://doi.org/10.1016/j.spacepol.2018.12.005>.
- [8] M. Shan, J. Guo, E. Gill, Deployment dynamics of tethered-net for space debris removal, *Acta Astronaut.* 132 (2017) 293–302.
<https://doi.org/10.1016/j.actaastro.2017.01.001>.
- [9] V. V Svotina, M. V Cherkasova, Space debris removal – Review of technologies and techniques . Flexible or virtual connection between space debris and service spacecraft, *Acta Astronaut.* (2022).
<https://doi.org/10.1016/j.actaastro.2022.09.027>.
- [10] A. Ledkov, V. Aslanov, Review of contact and contactless active space debris removal approaches, *Prog. Aerosp. Sci.* 134 (2022) 100858.
<https://doi.org/10.1016/j.paerosci.2022.100858>.
- [11] S. Kitamura, Large space debris reorbiter using ion beam irradiation, in: 61st Int. Astronaut. Congr. Prague, Czech Repub., 2010.
- [12] J.M. Ruault, M.C. Desjean, C. Bonnal, P. Bultel, Active Debris Removal (ADR): From identification of problematics to in flight demonstration preparation, in: 1st Eur. Work. Act. Debris Remov., 2010.
- [13] C. Bombardelli, J. Pelaez, Ion beam shepherd for contactless space debris removal, *J. Guid. Control. Dyn.* 34 (2011) 916–920.
<https://doi.org/10.2514/1.51832>.
- [14] C. Bombardelli, H. Urrutxua, M. Merino, E. Ahedo, J. Peláez, Relative dynamics and control of an ion beam shepherd satellite, *Adv. Astronaut. Sci.* 143 (2012) 2145–2157.

- [15] A.P. Alpatov, S.V. Khoroshylov, A.I. Maslova, Contactless de-orbiting of space debris by the ion beam. *Dynamics and Control, Akademperiodyka*, Kyiv, 2019. <https://doi.org/10.15407/akademperiodyka.383.170>.
- [16] A. Alpatov, S. Khoroshylov, C. Bombardelli, Relative control of an ion beam shepherd satellite using the impulse compensation thruster, *Acta Astronaut.* 151 (2018) 543–554. <https://doi.org/10.1016/j.actaastro.2018.06.056>.
- [17] S. Khoroshylov, Relative control of an ion beam shepherd satellite in eccentric orbits, *Acta Astronaut.* 176 (2020) 89–98. <https://doi.org/10.1016/j.actaastro.2020.06.027>.
- [18] V.M. Kulkov, N.N. Markin, Y.G. Egorov, Issues of controlling the motion of a space object by the impact of the ion beam, *IOP Conf. Ser. Mater. Sci. Eng.* 927 (2020). <https://doi.org/10.1088/1757-899X/927/1/012051>.
- [19] V.A. Obukhov, V.A. Kirillov, V.G. Petukhov, A.I. Pokryshkin, G.A. Popov, V.V. Svochina, N.A. Testoyedov, I.V. Usovik, Control of a service satellite during its mission on space debris removal from orbits with high inclination by implementation of an ion beam method, *Acta Astronaut.* 194 (2022) 390–400. <https://doi.org/10.1016/j.actaastro.2021.09.041>.
- [20] V. Aslanov, A. Ledkov, M. Konstantinov, Attitude dynamics and control of space object during contactless transportation by ion beam, *Proc. Int. Astronaut. Congr. IAC. 2020-October* (2020) 1–7.
- [21] V.S. Aslanov, A.S. Ledkov, Space debris attitude control during contactless transportation in planar case, *J. Guid. Control. Dyn.* 43 (2020) 451–461. <https://doi.org/10.2514/1.G004686>.
- [22] Y. Nakajima, H. Tani, T. Yamamoto, N. Murakami, S. Mitani, K. Yamanaka, Contactless space debris detumbling: A database approach based on computational fluid dynamics, *J. Guid. Control. Dyn.* 41 (2018) 1906–1918. <https://doi.org/10.2514/1.G003451>.
- [23] V. Aslanov, A. Ledkov, Detumbling of axisymmetric space debris during transportation by ion beam shepherd in 3D case, *Adv. Sp. Res.* (2021). <https://doi.org/10.1016/j.asr.2021.10.002>.

- [24] S. Kitamura, Y. Hayakawa, S. Kawamoto, A reorbiter for large GEO debris objects using ion beam irradiation, *Acta Astronaut.* 94 (2014) 725–735. <https://doi.org/10.1016/j.actaastro.2013.07.037>.
- [25] V.A. Obukhov, V.A. Kirillov, V.G. Petukhov, G.A. Popov, V.V. Svitina, N.A. Testoyedov, I.V. Usovik, Problematic issues of spacecraft development for contactless removal of space debris by ion beam, *Acta Astronaut.* 181 (2021) 569–578. <https://doi.org/10.1016/j.actaastro.2021.01.043>.
- [26] A. Barea, H. Urrutxua, L. Cadarso, Large-scale object selection and trajectory planning for multi-target space debris removal missions, *Acta Astronaut.* 170 (2020) 289–301. <https://doi.org/10.1016/j.actaastro.2020.01.032>.
- [27] M. Merino, Modeling the physics of plasma thruster plumes in electric propulsion, *ESAC Sci. Semin.* (2017). https://www.cosmos.esa.int/documents/13611/1287426/170126_Merino.pdf.
- [28] F.F. Gabdullin, A.G. Korsun, E.M. Tverdokhlebova, The Plasma Plume Emitted Onboard the International Space Station Under the Effect of the Geomagnetic Field, *IEEE Trans. Plasma Sci.* 36 (2008) 2207–2213. <https://doi.org/10.1109/TPS.2008.2004236>.
- [29] F. Cichocki, M. Merino, E. Ahedo, Spacecraft-plasma-debris interaction in an ion beam shepherd mission, *Acta Astronaut.* 146 (2018) 216–227. <https://doi.org/10.1016/j.actaastro.2018.02.030>.
- [30] IADC, IADC Space Debris Mitigation Guidelines, 3rd ed., 2021.
- [31] V.S. Aslanov, A.S. Ledkov, Fuel costs estimation for ion beam assisted space debris removal mission with and without attitude control, *Acta Astronaut.* 187 (2021) 123–132. <https://doi.org/10.1016/j.actaastro.2021.06.028>.
- [32] V.S. Aslanov, A.S. Ledkov, M.S. Konstantinov, Attitude motion of a space object during its contactless ion beam transportation, *Acta Astronaut.* 179 (2021) 359–370. <https://doi.org/10.1016/j.actaastro.2020.11.017>.
- [33] A. Alpatov, F. Cichocki, A. Fokov, S. Khoroshylov, M. Merino, A. Zakrzhevskii, Determination of the force transmitted by an ion thruster

- plasma plume to an orbital object, *Acta Astronaut.* 119 (2016) 241–251.
<https://doi.org/10.1016/j.actaastro.2015.11.020>.
- [34] J. Fisher, B. Ferraiuolo, J. Monheiser, K. Goodfellow, A. Hoskins, R. Myers, J. Bontempo, J. McDade, T. O'Malley, G. Soulas, R. Shastry, M. Gonzalez, NEXT-C Flight Ion System Status, in: *AIAA Propuls. Energy 2020 Forum*, American Institute of Aeronautics and Astronautics, Reston, Virginia, 2020: pp. 1–32. <https://doi.org/10.2514/6.2020-3604>.
- [35] M. Patterson, J. Foster, H. McEwen, D. Herman, E. Pencil, J. VanNoord, NEXT Multi-Thruster Array Test - Engineering Demonstration, in: *42nd AIAA/ASME/SAE/ASEE Jt. Propuls. Conf. & Exhib.*, American Institute of Aeronautics and Astronautics, Reston, Virginia, 2006: pp. 8187–8208. <https://doi.org/10.2514/6.2006-5180>.
- [36] J.-C. Liou, An active debris removal parametric study for LEO environment remediation, *Adv. Sp. Res.* 47 (2011) 1865–1876.
<https://doi.org/10.1016/j.asr.2011.02.003>.

Active space debris removal by ion multi-beam shepherd spacecraft

A.S. Ledkov¹, V.S. Aslanov^{2,*}Samara National Research University, Theoretical Mechanics Department,
Samara, Russia**Abstract**

Contactless transportation of a passive object by an ion beam generated by an active spacecraft's thruster is a promising way of space debris removal. The study proposes a modification of the ion beam shepherd concept using an array of impulse transfer thrusters. The multi-beam scheme provides significant increase the generated ion force, which reduces a space debris object deorbit time, thereby reducing the probability of its collision with other orbital objects. The aim of the work is to study the possibility of using several ion beams for effective contactless transportation of a space debris object. Controlling the angular motion of the object permits orientation of the object to maximize the generated ion force. The article proposes a control law for impulse transfer thrusters, which is based on the calculation of the energy of the object's unperturbed motion, and two control schemes that implement this law: (1) relay control, which implies turning the thruster on and off, and (2) ion beam axis direction control for one of the thrusters. For a space debris object of a cylindrical shape, a comparison of the time and fuel costs required for deorbiting the object using one, two, and three impulse transfer thrusters is made. It is shown that the addition of thrusters significantly reduces the descent time, but has little effect on the mass of required fuel. For the case of two engines, the best angle of ion beams axes direction and the most preferable angular motion mode are determined. Numerical simulation of space debris removal is carried out for the case when the space debris object is in the least favorable mode of angular motion and the proposed control schemes are used. The ion beam direction control

¹ E-mail address: ledkov@inbox.ru. Website: <http://www.ledkov.com>

* Corresponding author

² E-mail address: aslanov_vs@mail.ru. Website: <http://aslanov.ssau.ru>

scheme showed better results than the relay scheme. The use of multiple ion beams opens up new possibilities for creating new ion beam shepherd spacecraft design and developing new control methods and laws.

Keywords: space debris; ion beam; attitude motion; control law; contactless transportation; ion multi-beam shepherd

1. Introduction

The threat of space debris is one of the challenges facing modern practical astronautics. Scientists agree that the solution to this problem is not possible without active space debris removal, which consists in the use of active spacecraft to deorbit large space debris or to transport it to a disposal orbit. Since the beginning of space **activities**, the amount of space debris in Earth orbit has been increasing. **Maintaining the** existing approaches to the problem, the population of space debris will grow at an accelerated rate [1]. According to the estimates given in [2,3], it is necessary to remove at least 5 large space debris objects annually to stabilize the situation in orbit. Given the plans of commercial companies to deploy their constellations of satellites, this number should be increased [4]. Study [5] provides a list of the most dangerous space debris objects in low Earth orbit (LEO). Over the past two decades, the scientific community has proposed many different schemes, approaches and methods for large space debris removal. Review articles [6–10] provide insight into the current state of affairs in this area. One of the promising ways of space debris removal is contactless transportation by means of an ion beam created by the thruster of an active spacecraft. Particles of the plume of the thruster hit a space debris surface and generate a force. This force can be used for transportation purposes. This idea has been proposed independently by three groups of scientists [11–13]. The force that is generated in such way will be referred to as the ion force. The absence of direct mechanical contact between the active spacecraft and the space debris object makes this method safe, since the risk of an accident during capture or

docking is excluded, and insensitive to the angular motion parameters of the space debris object, which makes it possible to transport even rapidly rotating objects.

To date, there are a lot of works devoted to various aspects of contactless ion beam assisted transportation of space debris. Mathematical models describing the motion of space debris and an active spacecraft during the space debris removal mission in various assumptions are developed in works [14,15]. The control laws of the active spacecraft relative position are proposed in [14,16–19]. Ion beam control laws for space debris motion relative to its center of mass are developed in research [20,21]. Space debris detumbling using ion beam torque is considered in [22,23]. Studies [24–26] are devoted to planning a missions of ion beam assisted space debris removal. Features of the physics of the ion beam and its interaction with the surface of space debris are studied in works [27–29]. A detailed analysis of studies on the topic of ion beam assisted transportation can be found in Section 4.2 of the review paper [10].

One of the weak points of contactless transportation by ion beam is the relatively small value of the generated force. The low value of the ion force leads to the fact that the transportation takes quite a long time. This can increase the probability of a transported object colliding with space debris when passing through densely populated heights. According to existing guidelines [30], the descent of space debris to Earth should not pose an undue risk to people or property. Deorbiting large space debris from LEO involves a controlled re-entry, for which the generated ion force may not be large enough. The magnitude of this force can be increased by increasing the ion outflow velocity or its concentration, which will require the modernization of the used ion engines. The article proposes a modification of the ion beam shepherd concept, which consists in the simultaneous use of several ion beams generated by different thrusters. In addition to increasing the generated force, the use of several beams creates additional opportunities for controlling the attitude motion of the transported object. Research [31] showed that controlling the object's angular motion during its contactless transportation can increase the efficiency of the system by transporting the object in an angular mode corresponding to the

maximum generated ion force. It should be noted that the use of several ion thrusters to generate an ion beam was described in [24], where a large space debris reorbiting mission in GEO was simulated using an active spacecraft equipped with four thrusters.

The aim of the work is to study the possibility of using several ion beams for effective contactless transportation of a space debris object. A comparison of a space debris object removal from LEO using one, two and three thrusters (Fig. 1) will be made. A control law that ensures the transfer of a space debris object to a given angular motion mode will be proposed. Two schemes for controlling the active spacecraft's thrusters that implement the developed control law will be considered. An estimation of the savings in time and fuel when using angular motion control during the space debris object descent will be made.

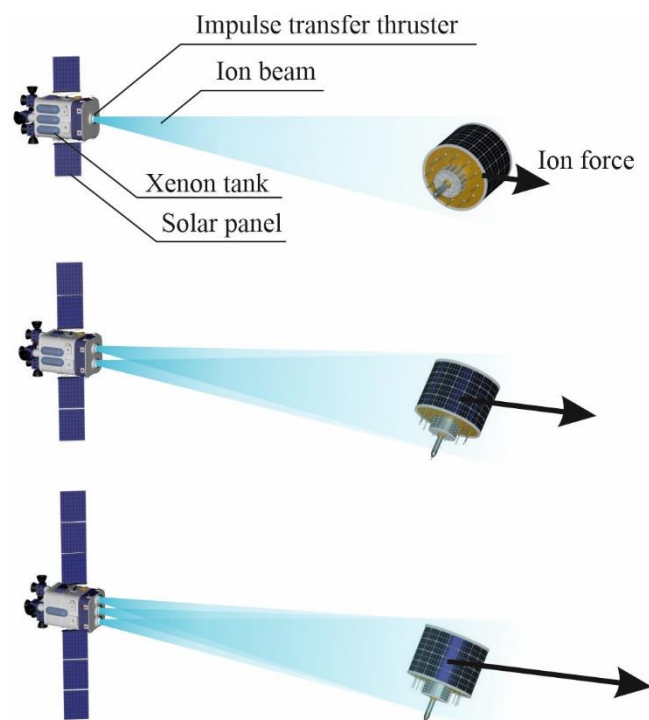


Fig. 1. Various active spacecraft designs.

During the study, several assumptions are made: the planar motion of the system is considered. It is assumed that the mutual influence of particles of intersecting ion beams is negligible due to the low concentration of particles in the plume and the high speed of their propagation. **According to the simulation results**

given in [29], the effect of the plasma environment on the value of the transferred ion force is negligible, since ion beam acts as potential barriers for the ambient plasma ions. The active spacecraft is considered as a material point, and the space debris object as a cylinder, the symmetry axis of which lies in the plane of the orbit. The center of mass of the cylinder is in its geometrical center. The motion occurs under the influence of only gravitational and ion forces and torques, as well as the thrust force of the control engines of the active spacecraft.

2. Mathematical model

2.1. Equations of motion

Consider the motion of a mechanical system consisting of a space debris object and an active spacecraft equipped with multiple impulse transfer thrusters, impulse compensation thrusters and control engines (Fig. 2). The equations of motion of the mechanical system do not differ from the conventional equations used to describe the motion of a system with a single ion impulse transfer thruster [32].

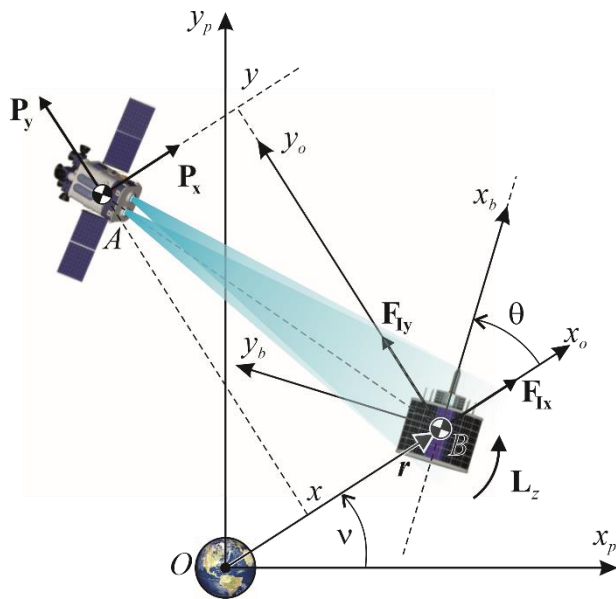


Fig. 2. Considered mechanical system.

$$\ddot{r} = \dot{v}^2 r - \frac{\mu}{r^2} + \frac{F_{Ix}}{m_B} + \frac{3\mu(3I_x \cos^2 \theta + 3I_y \sin^2 \theta - I_x - I_y + I_z)}{2m_B r^4}, \quad (1)$$

$$\ddot{v} = -\frac{2\dot{v}\dot{r}}{r} + \frac{F_{ly}}{m_B r} - \frac{3\mu(I_x - I_y)\sin\theta\cos\theta}{m_B r^5}, \quad (2)$$

$$\ddot{\theta} = \frac{L_z}{I_z} + \frac{2\dot{v}\dot{r}}{r} - \frac{F_{ly}}{m_B r} + \frac{3\mu(I_x - I_y)\sin\theta\cos\theta}{r^3} \left(\frac{1}{m_B r^2} + \frac{1}{I_z} \right), \quad (3)$$

$$\ddot{x} = \ddot{v}y - \ddot{r} + \dot{v}^2(r+x) + 2\dot{v}\dot{y} + \frac{P_x}{m_A} - \frac{\mu(r+x)}{r_A^3}, \quad (4)$$

$$\ddot{y} = \dot{v}^2 y - \ddot{v}(r+x) - 2\dot{v}(\dot{r} + \dot{x}) + \frac{P_y}{m_A} - \frac{\mu y}{r_A^3}. \quad (5)$$

where r is the space debris object position vector, r_A is the distance between the active spacecraft and the center of the Earth, v is the true anomaly angle, θ is the space debris axis deflection angle, x, y are the active spacecraft's coordinates in Local-vertical/local-horizontal reference frame (LVLH). The origin of this frame coincides with the center of mass of the space debris object (point B). The axis Bx_o is directed along \mathbf{r} , the axis By_o is perpendicular to Bx_o and directed to the orbital flight direction, m_A is the mass of the active spacecraft, m_B is the mass of the space debris, I_x, I_y , and I_z are the components of the inertia tensor of the space debris object, μ is the gravitational constant of the Earth, P_x, P_y are the components of the thrust force generated by the propulsion system of the active spacecraft, F_{lx}, F_{ly} are the components of the resultant ion force of the impulse transfer thrusters array, L_z is the resultant ion torque. The following equation is used to control the relative position of the active spacecraft.

$$P_x = k_x(x_A - x) - k_{dx}\dot{x}, \quad (6)$$

$$P_y = P_{y0} + k_y(y_A - y) - k_{dy}\dot{y}, \quad (7)$$

where x_A, y_A are the coordinates of the required relative position of the active spacecraft, k_j are control coefficients, is P_{y0} the thrust required to compensate for impulse transfer thruster.

2.2. Calculation of resultant ion force and torque for multi-beam shepherd spacecraft

To calculate the forces and torque generated by the ion beam, we use the calculation procedure described in detail in [33] and implemented by the authors in Matlab. The surface of the body is divided into triangles, after which the impact of the ion beam on each triangle is calculated. The flow parameters in the vicinity of the triangle are determined using the self-similar model of ion propagation. Assuming that, due to the low density, the particles of the intersecting ion beams do not influence each other, the total influence of N beams can be found as a geometric sum

$$\mathbf{F}_I = \sum_{j=1}^N \mathbf{F}_{Ij}(x, y, \theta, x_{Tj}, y_{Tj}, \beta_j), \quad \mathbf{L}_I = \sum_{j=1}^N \mathbf{L}_{Ij}(x, y, \theta, x_{Tj}, y_{Tj}, \beta_j) \quad (8)$$

where \mathbf{F}_{Ij} is vector of the force generated by the ion beam of the j -th impulse transfer thruster, \mathbf{L}_{Ij} is vector of ion torque generated by j -th thruster, x_{Tj} and y_{Tj} are the coordinates of the source of the j -th ion beam (P_j point on Fig. 3), β_j is the angle of the ion beam axis deviation from P_jB line connecting the center of mass of space debris and the j -th thruster (Fig. 3). The projections of the ion force on the axes of the orbital reference frame $Bx_o y_o$ can be found as

$$F_{Ix} = \sum_{j=1}^N (F_{Ijx} \cos \gamma_j + F_{Ijy} \sin \gamma_j), \quad F_{Iy} = \sum_{j=1}^N (F_{Ijy} \cos \gamma_j - F_{Ijx} \sin \gamma_j) \quad (9)$$

where $\cos \gamma_j = \frac{y_{Ti}}{\sqrt{x_{Ti}^2 + y_{Ti}^2}}$, $\sin \gamma_j = \frac{x_{Ti}}{\sqrt{x_{Ti}^2 + y_{Ti}^2}}$, F_{Ijx} and F_{Ijy} are calculated for single j -th impulse transfer thruster case when active spacecraft position is $x=0$, $y = \sqrt{x_{Tj}^2 + y_{Tj}^2}$ (Fig. 3b).

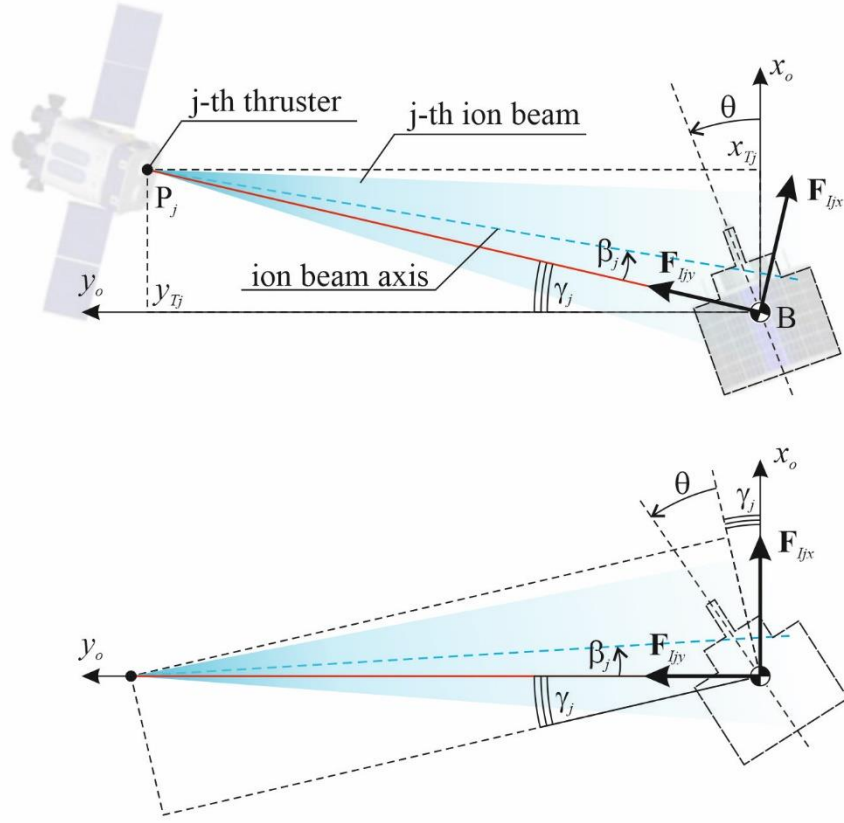


Fig. 3. Ion force components for j -th impulse transfer thruster.

To calculate the ion force generated of the j -th thruster \mathbf{F}_{ij} using the calculation procedure [33] it is required to know some ion beam parameters, in particular: the plasma density at the beginning of the far region of the ion beam n_0 , the ion velocity axial component u_0 , the ion beam divergence angle α_0 , the mass of the ion m_i , and the radius of the beam at the beginning of the far region R_0 . In scientific papers devoted to electric propulsion systems, these parameters are usually not given. Most often in such articles we can find total thruster input power P_{in} , total specific impulse I_{sp} , thrust F_T , and total efficiency η . Let's write down the expressions connecting the engine parameters with the parameters required for the calculation procedure. The ion velocity axial component can be approximately considered equal to the effective exhaust velocity of the thruster, which is

$$u_0 = V_{eff} = g_0 I_{sp}, \quad (10)$$

where $g_0 = 9.80665 \text{ m/s}^2$ is the Earth gravitational acceleration at sea level. The radius of the thruster nozzle can be used as the radius R_0 . The plasma density at the beginning of the far region for a thruster with a round nozzle can be approximately calculated as

$$n_0 = \frac{\dot{m}^2}{m_i \pi R_0^2 F_T}, \quad (11)$$

where \dot{m} is mass flow rate, which can be calculated as

$$\dot{m} = \frac{F_T}{I_{sp} g_0}, \quad (12)$$

or found from the expression for the total efficiency

$$\eta = \frac{F_T^2}{2\dot{m}P_{in}}. \quad (13)$$

Similar to the calculation of aerodynamic forces and torques, the calculation of ion forces and torques generated by an ion beam depends on the shape of the object placed in the ion beam and its orientation in the beam. Since the ion beam propagates in a rather narrow cone, the ion force and torque depend not only on the body orientation, but also on its position inside this cone, since, unlike aerodynamic forces, the parameters of the particle flow in its different parts are different. In addition, a part of the body may be outside of this cone. These circumstances make it much more difficult to model the motion of a body taking into account the impact of the ion beam. It is required either to perform a resource-intensive calculation of the ion force and torque at each integration step, or to approximate data from a pre-calculated database to obtain the force and torque values depending on the current position and orientation of the body. The latter approach is used, for example, in studies [22,31].

2.3. Ion multi-beam control schemes

Previous studies have shown that to control the angular motion of space debris, the most preferred method of control is to change the direction of the ion beam axis [21]. The controlled deflection of the beam allows the generation of an

ion torque, which tends to turn the object in the desired direction. With regard to an active spacecraft equipped with several impulse transfer thrusters, several control schemes can be proposed:

- 1) relay control based on turning on and off one of the thrusters;
- 2) changing the axis direction of one of the thrusters while maintaining the direction of the axes of other thrusters.

Regardless of which scheme is used, eventually the system is transferred to one of two states, which are characterized by the sign of the generated resultant ion torque over the entire range of angle θ (Fig. 4). After transferring the transported object to the required angular motion mode, the active spacecraft goes into the transportation mode, which implies the use of all impulse transfer thrusters.

To control an active spacecraft and switch between the states described above, it is proposed to use a control law based on an estimate of the energy of unperturbed motion. Such approach was used to control the direction of the axis of the ion beam of one thruster in the study [31]. Unperturbed motion is understood as the motion of a space debris object in a circular orbit under the action of an ion beam, when the active spacecraft occupies a constant relative position. In this case, equation (3) takes the form

$$\ddot{\theta} = \frac{L_z(\theta, s)}{I_z} + \frac{3\mu(I_x - I_y)\sin\theta\cos\theta}{I_z r^3}, \quad (14)$$

where s is the parameter that determines the state of the active spacecraft. The value $s = 0$ corresponds to the transportation mode, $s = 1$ corresponds to the case $L_z > 0$, and $s = 2$ corresponds to the case $L_z < 0$ (Fig. 4).

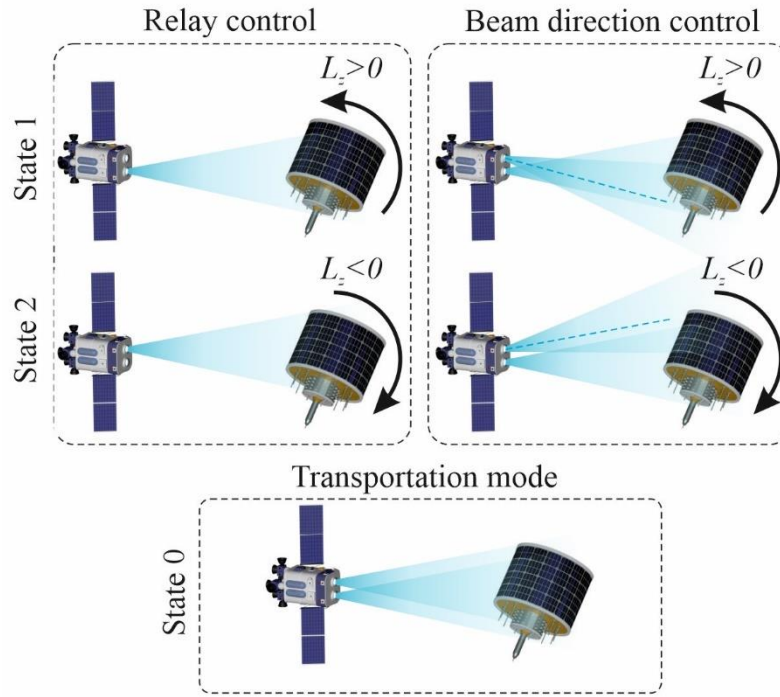


Fig. 4. Ion force components for j -th impulse transfer thruster.

For equation (14), the energy integral can be calculated as

$$E(\theta, \dot{\theta}, s) = \frac{\dot{\theta}^2}{2} - \frac{\int L_z(\theta, s) d\theta}{I_z} - \frac{3\mu(I_y - I_x) \cos 2\theta}{4I_z r^3}. \quad (15)$$

The considered unperturbed system is conservative and the energy E retains its value along each phase trajectory. If the phase portrait of the unperturbed system contains a separatrix that divides the phase plane into several oscillation regions, then one energy value can correspond to several phase trajectories located in different oscillation regions. In this case, the energy value E_* and the boundaries of the oscillation regions θ_1, θ_2 must be specified to identify the phase trajectory. Due to the conservatism of the unperturbed system $E(\theta_1, 0, 0) = E(\theta_2, 0, 0)$. In the absence of equilibrium positions, the energy uniquely determines the trajectory. The condition for the absence of an equilibrium position for equation (14) can be written as

$$|L_z(\theta, s)| > \frac{3\mu |I_x - I_y|}{2r^3} = L_{zmin}. \quad (16)$$

In the case when the perturbed motion of the system is considered, the orbit semi-latus rectum p can be taken instead of the radius r when calculating the energy (15) and limit value L_{zmin} in condition (16). For a mission of space debris removal in low Earth orbit, it is reasonable to take the radius of the atmosphere boundary as the radius r in condition (16). In this case, the condition $|L_z(\theta, s)| > L_{zmin}$ will also hold for higher orbits.

Consider the issue of transferring the system to an angular motion mode characterized by the energy $E_* = E(\theta_*, \dot{\theta}_*, 0)$, calculated by the equation (15), where $\dot{\theta}_*(\theta_*)$ is the required phase trajectory. The phase trajectory intersects the axis $\dot{\theta} = 0$ at the points θ_{*1} and θ_{*2} . If the target trajectory is the equilibrium position, then $\theta_{*1} = \theta_{*2} = \theta_*$. It is assumed that for State 1 ($s = 1$) and State 2 ($s = 2$) condition (16) is satisfied. In this case, the phase portrait and the dependence of the energy on the angle θ for States 1 and 2 are schematically shown in Fig. 5. To transfer the representative point of the system from an arbitrary state to the target trajectory, it is proposed to switch the state of the system in accordance with Table 1. In order to switch from one state to another in time, at each integration step, one should track the energies corresponding to states different from the current state and compare them with the conditions in Table 1.

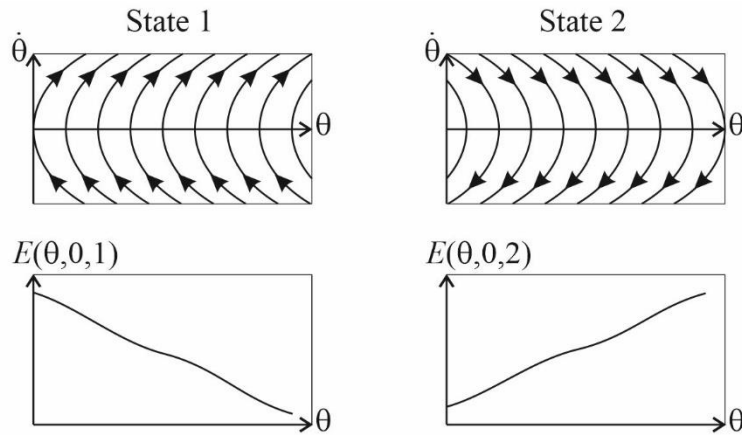


Fig. 5. Schematic representation of the phase portrait and energy for the case of controlled motion of space debris in States 1 and 2

Table 1. Control strategy

| Current angular velocity , $\dot{\theta}$ | Current energy, E | Control state, s (Fig. 4) |
|---|--|-----------------------------|
| $\dot{\theta} \leq 0$ | $E(\theta, \dot{\theta}, 1) < E(\theta_{*2}, 0, 1)$ | 2 |
| $\dot{\theta} \leq 0$ | $E(\theta, \dot{\theta}, 1) \geq E(\theta_{*2}, 0, 1)$ | 1 |
| $\dot{\theta} > 0$ | $E(\theta, \dot{\theta}, 2) < E(\theta_{*1}, 0, 2)$ | 1 |
| $\dot{\theta} > 0$ | $E(\theta, \dot{\theta}, 2) \geq E(\theta_{*1}, 0, 2)$ | 2 |
| $\dot{\theta} \in (-\infty, \infty)$ | $E(\theta, \dot{\theta}, 0) = E(\theta_{*1}, 0, 0)$ | 0 |
| Other cases | | 0 |

Fig. 6 schematically shows the translation of the imaging point in the phase space $(\theta, \dot{\theta})$ to the target trajectory using the described above approach. The yellow color shows the area where, according to Table 1, the spacecraft must be transferred to State 1. The area marked in blue is where the state should be set to State 2. Bold black lines on the boundary of the regions show the phase trajectories having energy $E(\theta_{*2}, 0, 1)$ and $E(\theta_{*1}, 0, 2)$ in States 1 and 2, respectively. The point A at the initial moment of time has an angular velocity $\dot{\theta} < 0$ and an energy $E(\theta, \dot{\theta}, 1) \geq E(\theta_{*2}, 0, 1)$. In this case, the conditions of the second row of Table 1 are met. After the trajectory passes the abscissa axis (point B), it enters the area $\dot{\theta} > 0$, where $E(\theta, \dot{\theta}, 2) < E(\theta_{*1}, 0, 2)$, and the conditions in the third row of Table 1 are met. At point C, the energy reaches the value $E(\theta, \dot{\theta}, 2) = E(\theta_{*1}, 0, 2)$, which means that the conditions of the fourth row from the table are satisfied. At this point, the system switches to State 2. Further motion occurs up to point θ_{*1} of the target trajectory, where $E(\theta, \dot{\theta}, 0) = E(\theta_{*1}, 0, 0) = E(\theta_{*2}, 0, 0)$ and the spacecraft is transferred to State 0. It should be noted that if the imaging point at the initial moment of time is inside the area limited by the target phase trajectory, then the transition to this trajectory can be carried out both by transferring the active spacecraft to State 1 and State 2.

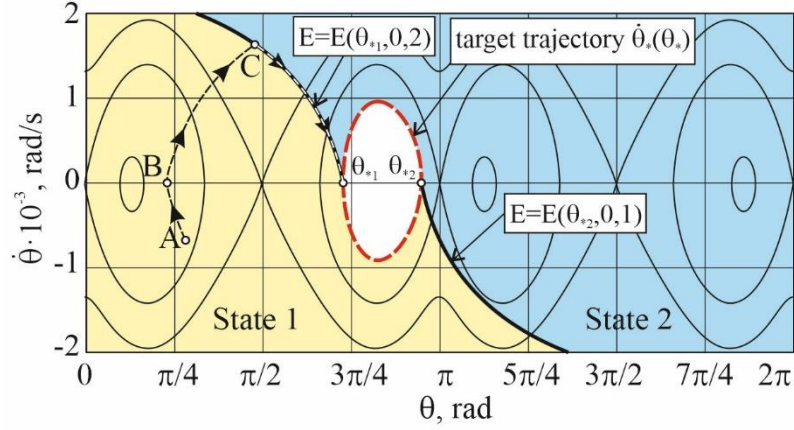


Fig. 6. Phase portrait for State 0 and various control areas

3. Numerical simulations

3.1. Fuel consumption for various thrusters' layouts

To evaluate the efficiency of using several ion beams to solve the problem of active space debris removal, let us simulate the space debris contactless transportation without controlling its attitude motion. In this subsection it is assumed that during the entire transportation, the axis of all impulse transfer thrusters passes through the center of mass of the space debris object. The control system of the active spacecraft keeps it in the relative position $x=0$, $y=15\text{m}$, so the distance between the transportation system and the space debris is 15m. The plane on which the impulse transfer thrusters' nozzles are located is perpendicular to the line AB connecting the centers of mass of the active spacecraft and the space debris object (Fig. 2).

Various cases are discussed below when the active spacecraft is equipped with one, two or three thrusters. The layout of engine nozzles on the surface of an active spacecraft is shown in Fig. 7. The displacement of the axis of the first and third engines from the axis is $h=0.5\text{m}$. The third column in Table 2 indicates which position of the thrusters corresponds to each of the considered cases. In our calculations, we will be guided by the NASA Evolutionary Xenon Thruster Commercial (NEXT-C) gridded ion thruster [34], the parameters of which are given

in Table 3. The ion beam parameters calculated using formulas(10)-(12), which are necessary for obtaining the ion forces and torque, are given in Table 4. In this study, the ion beam divergence angle is taken as 10 deg , since the authors could not find this parameter in the sources. Article [35] describes laboratory studies of the simultaneous operation of three NEXT thrusters. Research results show that the use of an array of thrusters does not lead to a decrease in the performance of each of them. Since the development of technology allows us to hope for the creation of more efficient engines, in addition to cases involving the use of one and several NEXT-like engines (cases 1-4), we will also consider cases of using a hypothetical engine that generates thrust equal to two and three NEXT engines (cases 5, 6). It is assumed that other parameters of the hypothetical thruster (nozzle radius, specific impulse) are the same as those of the array thruster.

Table 2. Compared cases

| Case | Number of thrusters | Thrusters' locations (Fig. 7) | Total thrust, mN | Required Power kW | Mass of fuel consumed, kg | Mission time, hours |
|------|---------------------|-------------------------------|------------------|-------------------|---------------------------|---------------------|
| 1 | 1 | 2 | 235 | 7.33 | 85.68 | 1949.5 |
| 2 | 2 | 1,2 | 470 | 14.66 | 86.08 | 978.9 |
| 3 | 2 | 1, 3 | 470 | 14.66 | 86.01 | 978.8 |
| 4 | 3 | 1,2,3 | 705 | 21.99 | 86.14 | 653.6 |
| 5 | 1 | 2 | 470 | 14.66 | 85.90 | 977.6 |
| 6 | 1 | 3 | 705 | 21.99 | 86.02 | 652.7 |

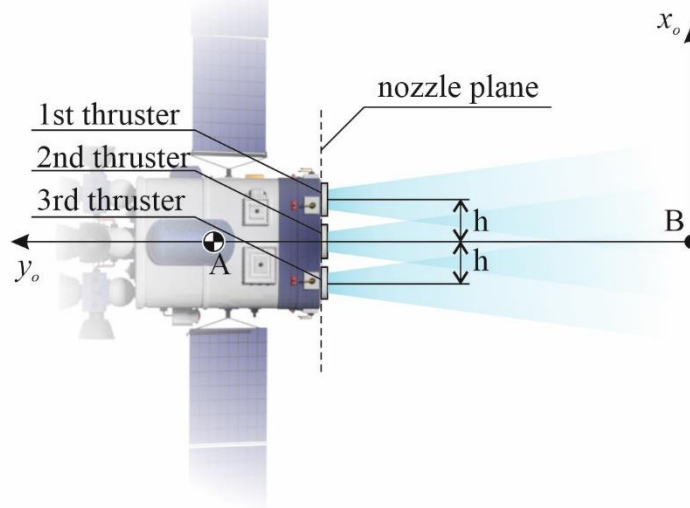


Fig. 7. Impulse transfer thrusters' location

Table 3 - NEXT-C parameters

| Parameter | Values |
|--------------------------------------|---------|
| Input power P_{in} | 7.33 kW |
| Thruster efficiency η | 0.7 |
| Thrust F_T | 235 mN |
| Specific impulse I_{sp} | 4155 s |
| Nozzle radius R_0 | 0.18 m |
| Ion thruster mass m_{IT} | 14 kg |
| Power processing unit mass m_{PPU} | 36 kg |

Table 4 - Ion beam parameters

| Parameter | Values |
|--------------------------------|---------------------------------------|
| Velocity axial component u_0 | 40747 m/s |
| Plasma density n_0 | $6.3787 \cdot 10^{15} \text{ m}^{-3}$ |
| Mass flow rate \dot{m} | $5.7673 \cdot 10^{-6} \text{ kg/s}$ |

| | |
|-----------------------------|---------------------------------|
| Xenon ion mass m_i | $2.18 \cdot 10^{-25} \text{kg}$ |
| Divergence angle α_0 | 10deg |

As an example, let us consider the removal of the Vostok second stage (SL-3), which mass is 1440 kg, length is 3.8 m, radius is 1.3 m [36]. It is assumed that the stage is a cylinder, the center of mass of which is located in its geometric center. The moments of inertia are calculated for an ideal cylinder case. The longitudinal moment of inertia is $2434 \text{ kg} \cdot \text{m}^2$, and the transverse moment of inertia is $1733 \text{ kg} \cdot \text{m}^2$. The stage moves in an elliptical orbit with an apoapsis height of 737 km and a periapsis height of 666.4 km. Figs. 8-10 show the dependences of the projections of the resultant ion force and torque on the axis of the orbital coordinate system, calculated for various ways of placing the thrusters given in Table 2. The shift of curve 2 in Fig. 8 to the negative area from other curves is due to the asymmetry of the thrusters' location in Case 2. As can be seen from Figs. 9 and 10, an increase in the total thrust of the engine array leads to an increase in the magnitude of the generated ion force and torque. In this case, the points of intersection of the curves L_z with the abscissa axis, which in the absence of a gravity gradient torque are the positions of equilibrium for the angle θ , remain unchanged in Cases 1, 3-6 and displaced very slightly in Case 2.

Let us simulate the descent of the stage until the moment when the periapsis height of its orbit drops to an altitude of 100 km using equations (1)-(5). In all cases it is assumed that the initial mass of the spacecraft is $m_{A0} = 700 \text{kg}$, of which $m_{f0} = 200 \text{kg}$ is the fuel reserve. The following initial conditions are used in the simulation

$$r_0 = 7037400 \text{m}, \dot{r}_0 = 0, v_0 = 0, \dot{v} = 1.0668 \cdot 10^{-3} \text{ rad/s}, \theta_0 = 3.84 \text{rad}, \dot{\theta}_0 = 0, x_0 = 0, \\ \dot{x}_0 = \dot{y}_0 = 0, y_0 = 15 \text{m}.$$

The diameter of the ion beam at the center of mass of the stage in the case of one thruster is 5.29m. The ratio of the beam diameter to the stage length is 1.39. The following values are taken as parameters of control laws (6)-(7)

$$k_x = k_y = 1000 \text{ kg/s}^2, k_{dx} = k_{dy} = 1000 \text{ kg/s}, P_{y0} = -0.247 F_T \frac{m_A}{m_B}$$

where F_T is the thrusters' array total thrust given in fourth column of Table 2. The use of control laws (6)-(7) requires tracking the relative position and relative velocity of the active spacecraft. To simulate the change in mass of the active spacecraft $m_A = m_{A0} - m_f$, the following differential equation is used

$$\dot{m}_f = \frac{2NF_T}{I_{sp}g_0} + \frac{|P_x| + |P_y|}{I_{sp}g_0}, \quad (17)$$

where m_f is mass of the fuel consumed. The factor 2 in the first term of equation (17) is due to the need to compensate for thrust of the spacecraft's impulse transfer thrusters by an additional compensation thrusters. For simplicity, it is assumed that the specific impulses of all spacecraft's thrusters are the same.

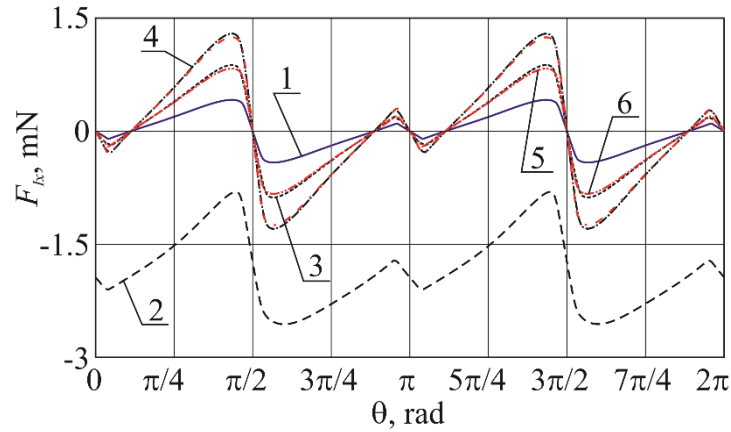


Fig. 8. Dependence of ion force projection F_{lx} on the deflection angle θ

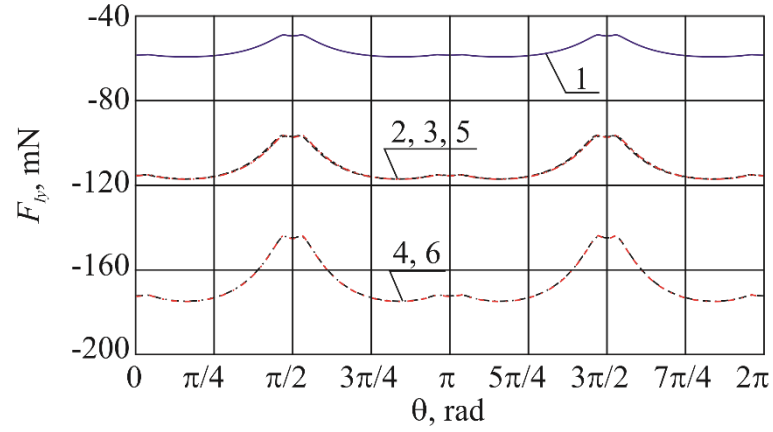


Fig. 9. Dependence of ion force projection F_y on the deflection angle θ

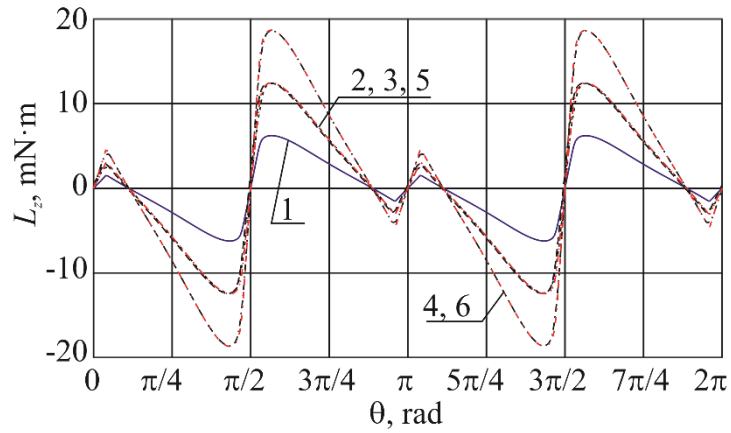


Fig. 10. Dependence of ion torque projection L_z on the deflection angle θ

Calculations show that in all simulated cases, the space debris object oscillates around the equilibrium position throughout the entire descent. The two right columns of Table 2 show the mass of fuel and the time of descent. A multiple increase in thrust leads to a significant decrease in the descent time. Despite the fact that the operating time of the thrusters is reduced, the installation of an additional thrusters increases fuel consumption per unit of time. As cases 2-4 show (Table 2), adding a thruster leads to an increase in the mass of fuel consumed compared to case 1, which implies the use of a single thruster. Comparing cases 2 and 3, it can be concluded that the asymmetrical placement of the thrusters does not lead to a significant change in the mass of the required fuel. It should be noted that in all cases, changes in mass are insignificant and do not exceed 0.46 kg.

3.2. Choice of angles of inclination of the ion beam axes

To investigate the influence of the angle of ion beam axis deviation on the magnitude of the generated ion force, let us perform a series of numerical calculations. It is assumed that the active spacecraft is equipped with two thrusters located symmetrically in accordance with Case 3 from Table 2. We restrict ourselves to the study of the case when the axes of the thrusters are rotated symmetrically by the angles β and $-\beta$, respectively. Fig. 11 shows the dependence of the projection of the ion force F_{ly} for various values of the angle β . The maximum value of ion force corresponds to the angle $\beta = -1.9^\circ$ when the ion beam axes pass through the geometric center of the cylinder. Fig. 12 demonstrates a bifurcation diagram showing the change in the equilibrium positions of the angle θ with a change in the angle β . This diagram is built using equation (14) for the case of a circular orbit. The phase portrait for the case $\beta = -1.9^\circ$ and a height of the circular orbit of 500 km is shown in Fig. 13. Center-type equilibrium positions correspond to a black solid line on the bifurcation diagram (Fig. 12), and unstable saddle points correspond to a red dashed line.

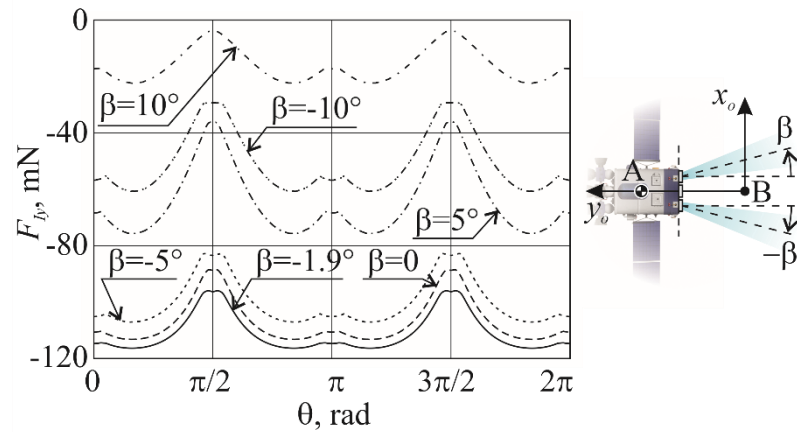


Fig. 11. Dependence of ion force projection F_{ly} on the deflection angle θ

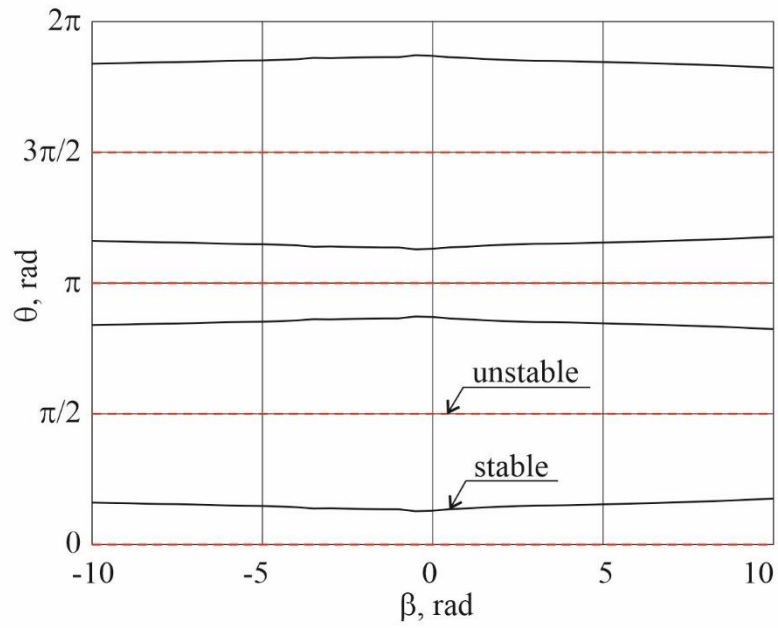


Fig. 12. Bifurcation diagram

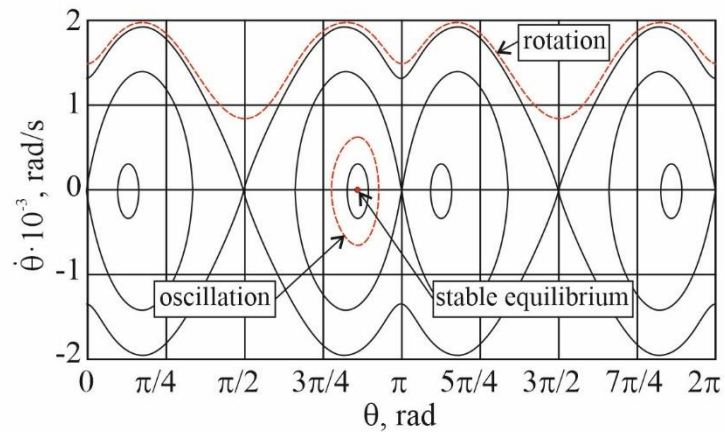


Fig. 13. The dependence of the mass of spent fuel on time

3.3. Choice of the most preferred angular motion mode of space debris

According to the phase portrait shown in Fig. 13, in the case of unperturbed motion corresponding to motion in a circular orbit under the action of an ion beam, a space debris object can perform angular motion related to one of three types: be in a position of stable equilibrium, oscillate or rotate. In the last two cases, the angle of the object deflection θ from the local vertical is constantly changing, which leads to a change in the force generated by the ion beam. The average ion force \bar{F}_y calculated on the period of the object's oscillations T can be used as a measure of

the effectiveness of the angular motion mode for the considered mission of contactless transportation

$$\bar{F}_{Iy} = \frac{1}{T} \int_0^T F_{Iy}(\theta(t)) dt. \quad (18)$$

Fig. 14 shows a graph of the average force dependence on angle θ_0 . For each value of θ_0 , a numerical calculation was carried out. Equation (14) was integrated for the initial conditions $\theta(0) = \theta_0$, $\dot{\theta}(0) = 0$ and then the average force was calculated using (18). Case 3 (Table 2), when two engines are used and the ion beam axes pass through the geometric center of the object, was used for the calculation.

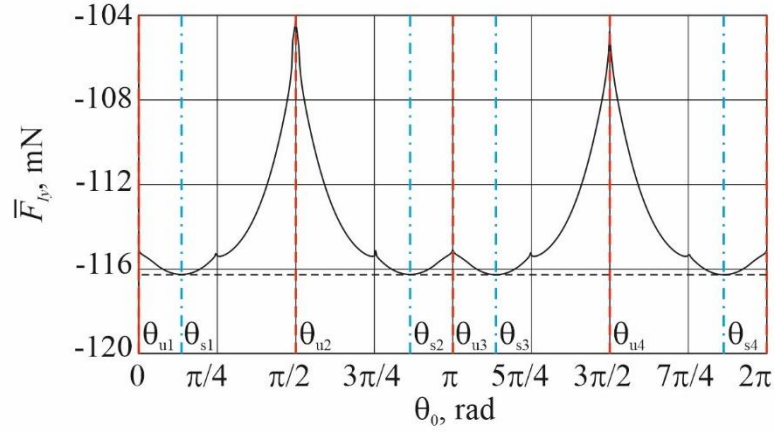


Fig. 14. The dependence of the average ion force projection on the space debris object deflection angle θ_0

Calculations show that for the considered case, the most favorable is transportation in a stable equilibrium position θ_{sj} . These positions are shown in Fig. 14 by blue dash-dotted lines. The maximum magnitude of the force is $\bar{F}_{Iy \max} = |\min_{\theta_0 \in [0, 2\pi]} \bar{F}_{Iy}(\theta_0)| = 0.1163 \text{ N}$. The minimum magnitude of the average force $\bar{F}_{Iy \min} = |\max_{\theta_0 \in [0, 2\pi]} \bar{F}_{Iy}(\theta_0)| = 0.1043 \text{ N}$ is observed in unstable positions θ_{s2} and θ_{s4} , when the object is oriented with a flat end surface to the flow. The values of the average force at the points of local minima and maxima coincide due to the symmetry of the ion beams and the considered space debris object. Fig. 15 shows the dependence of the average ion force on the initial angular velocity, for the case

of rotation. Integration was carried out under initial conditions $\theta(0) = \pi / 2$, $\dot{\theta}(0) = \dot{\theta}_0$. As the angular velocity increases, the averaged ion force tends to the value $\bar{F}_{ly} = -0.111\text{N}$.

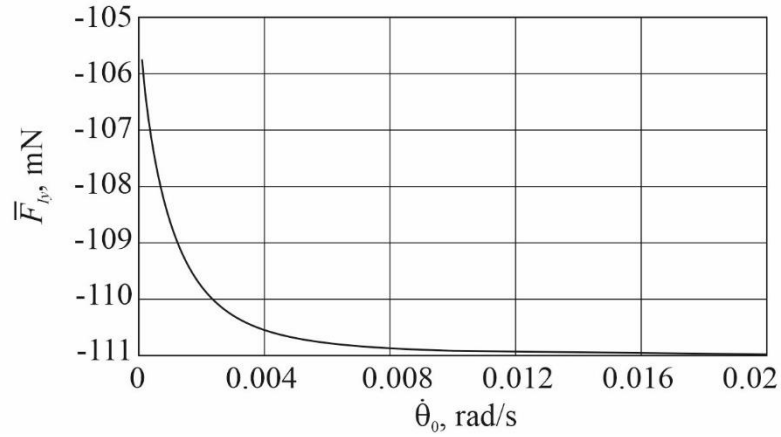


Fig. 15. The dependence of the average ion force projection on the space debris angular velocity $\dot{\theta}_0$

Comparing Figs. 14 and 15, it can be concluded that transportation in the oscillation mode and in the position of a stable equilibrium is more efficient in terms of the magnitude of the generated ion force than in the rotation mode. Numerical simulations of the most favorable and unfavorable regimes using equations (1)-(5), when the space debris object is in equilibrium positions $\theta_0 = 3.5655\text{rad}$ and $\theta_0 = \pi / 2$, respectively, show that in the favorable case, the mission lasts 974.0 hours and requires 85.61 kg of fuel, and in the unfavorable case, the required time and fuel consumption increase to 1055.1 hours and 92.35 kg. Taking the unfavorable case as 100%, when the object is transferred to a stable equilibrium position, the fuel savings are 7.3%.

3.4 Space debris attitude motion control

Consider the case when the space debris object is in an unfavorable angular regime determined by the initial conditions $\theta_0 = \pi / 2$, $\dot{\theta}_0 = 0$. The goal of control is to transfer the space debris object to position θ_{s3} (Fig. 14), corresponding to a

favorable regime. As in the previous subsection, it is assumed that the active spacecraft is equipped with two impulse transfer thrusters located in positions corresponding to Case 3 from Table 2. In accordance with the results of Section 3.2, the ion beams axes are directed towards the geometric center of the space debris object to provide the most efficient contactless transportation mode. Consider the two control schemes described in Section 2.3. Relay control of impulse transfer thrusters assumes that the axes of the ion beams cannot change their direction. Angular motion control is achieved by turning the thrusters on and off. Ion beam axis direction control assumes that one of the impulse transfer thrusters (thruster 1 in Fig. 7) is installed on a swiveling platform and can turn relative to the active spacecraft using an electric motor. The second thruster constantly maintains the direction of the axis of its beam.

To implement the control law described in Section 2.3, the ion torque in State 1 and 2 must satisfy the inequality (16). For the considered space debris, the ion torque limit value is $L_{zmin} = 0.0015 \text{ Nm}$.

3.4.1. Relay control of impulse transfer thrusters

Calculations of the dependence of the ion torque on θ for the case of operation of one of the two thrusters show that in the case when the beam axis is directed to the geometric center ($\beta = -1.9^\circ$), condition (16) is not fulfilled and the control scheme described in Section 2.3 cannot be implemented. Increasing the angle β , which determines the direction of the ion beam axis, solves this problem, but increasing the angle leads to a decrease in the generated ion force (Fig. 11), which in turn reduces the efficiency of the ion transportation system and leads to an increase in time and fuel costs. When the value of the angle $\beta = -0.4^\circ$ condition (16) is fulfilled (Fig. 16). The black solid line in Fig. 16 indicates the resultant ion torque generated by the two thrusters in positions 1 and 3 (Fig. 7). The red dashed lines in Fig. 16 correspond to the ion torques generated by the thruster in position 1. The blue dash-dotted lines show ion torques of thruster in position 3.

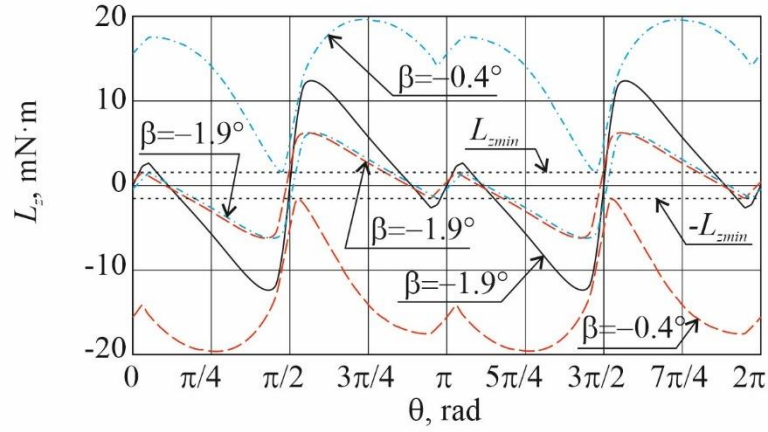


Fig. 16. Dependence of ion torque projection L_z on the deflection angle θ .

Consider a controlled descent of space debris at ion beam axis deflection angle $\beta = -0.4^\circ$. An active spacecraft can be in one of three states. In State 0, both impulse transfer thrusters are turned on. In State 1, only the thruster in position 3 is turned on, resulting in a positive ion torque. In State 2, only the thruster in position 1 is turned on, and a negative ion torque is generated. Fig. 17 demonstrates the phase trajectories for a space debris object using various control schemes. The relay control trajectory is shown by the red line. At the initial moment of time, the system is in the area where State 1 should be used. At point A_1 (Fig. 17), in accordance with the control law described in Section 2.3, the system switches to State 2. At point B_1 , the phase trajectory reaches the target equilibrium position and both engines turn on, bringing the system to State 0. Due to the fact that the considered system is not unperturbed, the representative point will not remain in the equilibrium position, but will oscillate around it with a small amplitude. Calculations show that the displacement of the representative point from the position to which the point was transferred using relay control at the initial stage of transportation does not exceed 0.035 rad (Fig. 17). The entire descent operation takes 990.3 hours and requires 86.96 kg of fuel. It should be noted that the values obtained for time and fuel turn out to be worse than those obtained in Section 3.3 for the case when the object is immediately in a favorable angular position. This deterioration is due to the fact that

angle β in this calculation has been changed, the beams axes do not pass through the center of mass of the object resulting in a decrease in ion force.

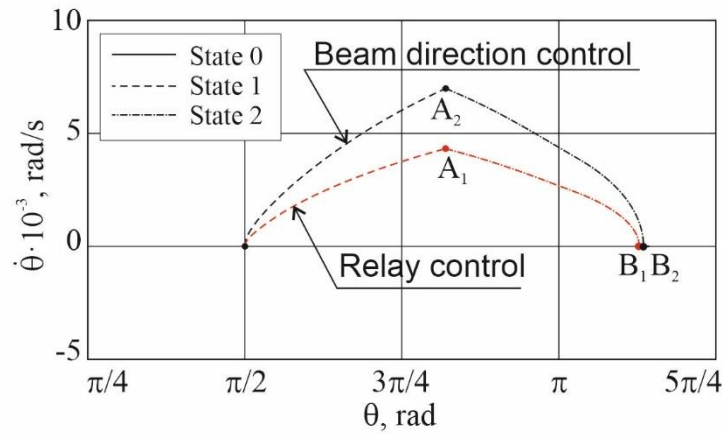


Fig. 17. Phase portraits for the case of controlled descent.

3.4.2. Ion beam axis direction control

A series of calculations using the procedure described in Section 2.2 was carried out. The goal was to determine the angles β of the first thruster's axis deflection corresponding maximum and minimum of the ion torque in States 1 and 2. Fig. 18 shows the dependences of the maximum and minimum resulting ion torque of two thrusters in positions 1 and 3 (Fig. 7) on the β angle of the first thruster. The maximum positive and minimum negative ion torque is observed at angles $\beta_1 = -8^\circ$ and $\beta_2 = 4.25^\circ$, respectively. Fig. 19 shows the corresponding dependences of the ion torques on the deflection angle of the space debris object θ .

Let's simulate a controlled descent of a space debris object using the first impulse transfer thruster to control the orientation of the object. The simulation assumes that the thruster's axis turns instantly. This is quite justified, since the period of the object's angular oscillations and the period of its orbital motion exceed 30 minutes, while the process of turning the platform with the thruster takes seconds. At the initial stage of motion, the object is in the area corresponding to State 1, so the first thrusters deviates by an angle β_1 . The phase trajectory is shown in Fig. 17 as a black line. At point A_2 , the energy $E(\theta, \dot{\theta}, 2)$ reaches the value $E(\theta_*, 0, 2)$ and,

in accordance with the fourth line of Table 1, the system is switched to State 2. To do this, the first thruster rotates through an angle β_2 . At point B_2 , the phase trajectory reaches the target equilibrium position, the axis of the first engine is directed to the center of mass of the object ($\beta = -1.9^\circ$), and the system switches to State 0. Mismatch of points B_1 and B_2 in Fig. 17 is due to the mismatch of β angles in State 0 in the case of relay control and beam axis control. Calculations show that for the implementation of the transport operation for the space debris object descent from orbit, 974.1 hours and 85.61 kg of fuel are required. These values are slightly worse than those obtained in Section 3.3 when the object is immediately in a favorable angular position.

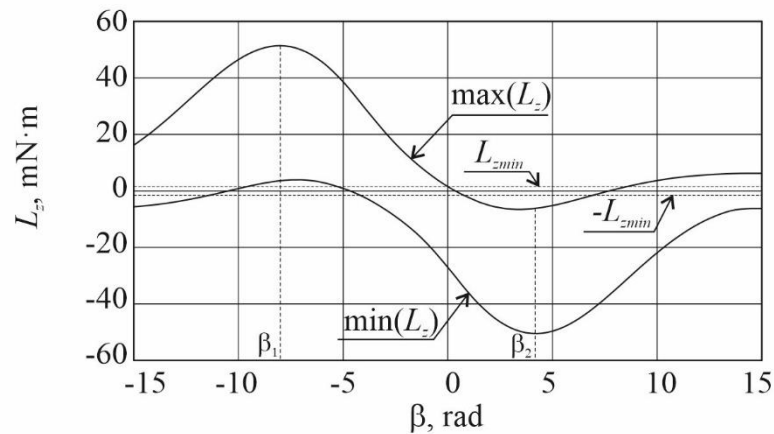


Fig. 18. Dependence of amplitude values of resulting ion torque L_z on the angle β , which determines the deviation of the axis of the ion beam of the first thruster.

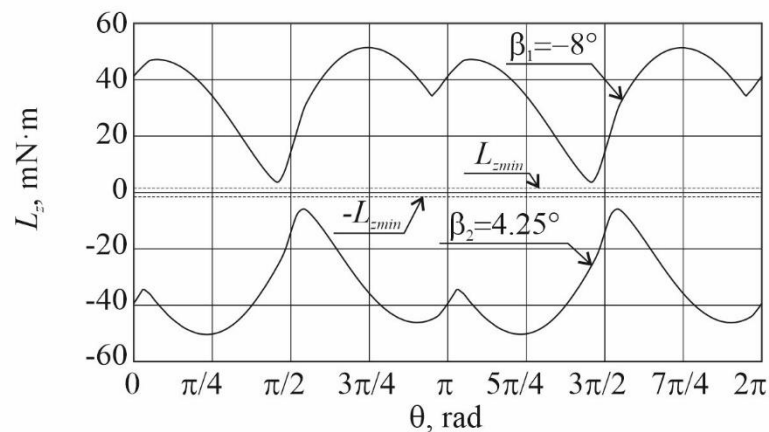


Fig. 19. Dependence of ion torque projection L_z on the deflection angle θ .

4. Discussion

As part of the study, a large number of numerical calculations were performed. The results are collected in a summary Table 5 for visual presentation. **The values given in the mass column include the cost of the impulse transfer thrusters, the impulse compensation thrusters and the control engines.** Obviously, using an array of impulse transfer thrusters does not result in fuel mass savings compared to using a single thruster. At the same time, an increase in the number of engines leads to a multiple decrease in the descent time, which can be of decisive importance for a space debris removal mission. Reducing the time of an object existence in orbit reduces the probability of **its** collision with other objects. Since the mass of required fuel does not change much when using a different number of engines, the failure of one of them does not lead to mission failure. The mission can be completed with one thruster, it just takes more time.

Table 5 – Summary of calculations results

| Case | Number of thrusters | Thrusters' locations (Fig. 7) | Total thrust, mN | Initial angle θ_0 , rad | Attitude control | Section | Mass of fuel consumed, kg | Mission time, hours |
|------|---------------------|-------------------------------|------------------|--------------------------------|------------------------|---------|---------------------------|---------------------|
| 1 | 1 | 2 | 235 | 3.84 | Uncontrolled | 3.1 | 85.68 | 1949.5 |
| 2 | 2 | 1,2 | 470 | 3.84 | Uncontrolled | 3.1 | 86.08 | 978.9 |
| 3 | 2 | 1, 3 | 470 | 3.84 | Uncontrolled | 3.1 | 86.01 | 978.8 |
| 4 | 3 | 1,2,3 | 705 | 3.84 | Uncontrolled | 3.1 | 86.14 | 653.6 |
| 5 | 1 | 2 | 470 | 3.84 | Uncontrolled | 3.1 | 85.90 | 977.6 |
| 6 | 1 | 3 | 705 | 3.84 | Uncontrolled | 3.1 | 86.02 | 652.7 |
| 7 | 2 | 1,3 | 470 | 3.5655 | Uncontrolled | 3.3 | 85.68 | 974.0 |
| 8 | 2 | 1,3 | 470 | 1.5708 | Uncontrolled | 3.3 | 92.35 | 1055.1 |
| 9 | 2 | 1,3 | 470 | 1.5708 | Relay control | 3.4.1 | 86.96 | 990.3 |
| 10 | 2 | 1,3 | 470 | 1.5708 | Beam direction control | 3.4.2 | 85.61 | 974.1 |

Calculations shown that the use of additional thrusters does not entail a significant change in the mass of fuel, however, their installation leads not only to an increase in the generated ion force, but also to an increase in the mass of the entire propulsion system of an active spacecraft. For a given mass budget, this means a reduction in the mass of propellant that a spacecraft can carry. The use of an additional engine also requires additional power consumption. This can also lead to an increase in spacecraft's dry mass due to the installation of additional segments of solar panels and batteries (Fig. 1). **An increase in the active spacecraft size due to the installation of additional solar arrays will increase the likelihood of its collision with other space debris during transportation. In this study it was assumed that the system is in "clean" space and there is no need to perform collision avoidance maneuvers. Trajectory planning taking into account the orbital motion of other objects will increase the time and cost of the removal operation.** These circumstances should be analyzed in detail when **developing the design of the active spacecraft** and preparing a multipurpose mission of active space debris removal.

Calculations show that the development and use of a more advanced impulse engine that generates more thrust while maintaining the specific impulse does not lead to a qualitative improvement in the required time and fuel mass compared to using an array of thrusters. One of the possible advantages of using a single thruster compared to an array is the absence of efficiency losses in the force generated on the surface of the transported object as a result of the interaction of particles in the beams of different thrusters. In carrying out this study, the mutual influence of intersecting ion beams on each other was not taken into account. This issue requires careful study, requiring laboratory experiments and detailed modeling of the interaction of thrusters' plumes. As a result of such studies, loss factors can be determined, which should be used in calculating the generated ion force and torque.

The results obtained in Section 3 apply only to the Vostok second stage in the case when the center of mass coincides with its geometric center. For objects of other geometry and layout, ion force and torque must be recalculated. A change in these force and torque will entail a change in the equilibrium positions and the location of

the most favorable and unfavorable modes of the object's angular motion for contactless transportation. The boundary value of the ion torque (16), which determines the possibility of using the method of controlling the angular position of an object described in Section 2.3, will also change.

The results of numerical simulation showed that the control law for the angular position of a transported object, proposed in Section 2.3, based on calculating the energy in the unperturbed case of a circular orbit, also works well for orbits with a small eccentricity. The possibility of using this scheme for orbits with a large eccentricity requires additional research, which involves identifying the limits of applicability of the control law and its possible modification.

The article considers two ways to control the transported object angular motion: relay control, which involves turning the thrusters on and off, and controlling the direction of the beam of one of the thrusters. The first method is simpler in terms of technical implementation, since it does not require modification of the active spacecraft design. The second method showed the best efficiency, but its implementation requires the installation of a thruster on a rotating platform, which is controlled by an electric motor. The transient time, over which the object is transferred from the initial to the target angular position, in the first and second schemes is 1051 s and 659 s, respectively. The lower efficiency of the first method is due to the need to increase the angle β to fulfill condition (16). As a result, after the system is transferred to the equilibrium position, the generated ion force turns out to be less than in the case where the beams axes pass through the object's center of mass. An alternative to increasing the β angle could be to move the active spacecraft along the By_o axis closer or farther to the space debris object while maintaining the direction of the ion beam axes. However, when the distance between the active spacecraft and the object changes, the equilibrium positions also change, which makes it impossible to use the proposed control law and requires its significant modification. Section 3.4 investigates the case when the active spacecraft is equipped with two impulse transfer thrusters. The use of more thrusters may require modification of the control scheme, determination of an effective way of

positioning and orienting the thrusters, taking into account the characteristics of the transported object.

5. Conclusion

The paper proposes a modification of the ion beam shepherd concept by using array of thrusters. Using several ion beams allows to increase generated resultant ion beam force. A plane case of motion of a mechanical system consisting of an active spacecraft and a cylindrical space debris object is considered. A control law for the impulse transfer thrusters of an active spacecraft based on the calculation of the energy of a space debris object unperturbed oscillations is proposed. The control law ensures the transfer of the space debris object to the required angular mode of motion. Two control schemes are proposed that use the developed control law: relay control based on turning on and off one of the thrusters; and ion beam axis direction control of one of the thrusters while maintaining the direction of the axes of other thrusters. An analytical condition for the ion torque, which must be satisfied in order to be able to implement the developed control law, is obtained. A numerical study of the removal of cylindrical space debris from low Earth orbit for a different number and location of ion thrusters is carried out. For the case of two symmetrically located thrusters, the influence of the angle of deviation of the ion beam axis from the line connecting the centers of mass of the active spacecraft and space debris on the value of the generated ion force is studied. The most favorable and unfavorable angular motion modes of space debris object are revealed. Numerical simulation of the system's controlled motion, which ensures the transfer of a space debris object from an unfavorable to a favorable angular motion mode, is carried out using proposed control schemes and law. Calculations have shown that the control scheme based on changing the direction of the ion beam of one of the thrusters is more efficient than relay control scheme. The transition process takes less time, and the entire space debris removal mission requires less fuel and time. For the considered case, the fuel savings in the case of relay control and beam direction control compared to

uncontrolled descent in an unfavorable angular mode are 5.8% and 7.3% respectively.

The use of an array of impulse transfer thrusters improves the environmental safety of the system, since it reduces the time required to complete the space debris removal mission, and also increases the reliability of the system, since the failure of one of the thrusters does not lead to mission failure. Controlling the angular motion of a space debris object makes it possible to reduce time and fuel costs. The use of multiple ion beams can be effective for contactless transportation of large objects of complex shape. It opens up new possibilities for creating new ion beam shepherd spacecraft design and developing new control methods and laws.

Acknowledgments

This study was supported by the Russian Science Foundation (Project No.22-19-00160).

References

- [1] H.G. Lewis, Understanding long-term orbital debris population dynamics, *J. Sp. Saf. Eng.* 7 (2020) 164–170. <https://doi.org/10.1016/j.jsse.2020.06.006>.
- [2] J.-C. Liou, N.L. Johnson, N.M. Hill, Controlling the growth of future LEO debris populations with active debris removal, *Acta Astronaut.* 66 (2010) 648–653. <https://doi.org/10.1016/j.actaastro.2009.08.005>.
- [3] C. Bonnal, J.M. Ruault, M.C. Desjean, Active debris removal: Recent progress and current trends, *Acta Astronaut.* 85 (2013) 51–60. <https://doi.org/10.1016/j.actaastro.2012.11.009>.
- [4] A. Rossi, A. Petit, D. McKnight, Short-term space safety analysis of LEO constellations and clusters, *Acta Astronaut.* 175 (2020) 476–483. <https://doi.org/10.1016/j.actaastro.2020.06.016>.
- [5] D. McKnight, R. Witner, F. Letizia, S. Lemmens, L. Anselmo, C. Pardini, A. Rossi, C. Kunstadter, S. Kawamoto, V. Aslanov, J.-C. Dolado Perez, V. Ruch, H. Lewis, M. Nicolls, L. Jing, S. Dan, W. Dongfang, A. Baranov, D.

- Grishko, Identifying the 50 statistically-most-concerning derelict objects in LEO, *Acta Astronaut.* 181 (2021) 282–291.
<https://doi.org/10.1016/j.actaastro.2021.01.021>.
- [6] H. Hakima, M.R. Emami, Assessment of active methods for removal of LEO debris, *Acta Astronaut.* 144 (2018) 225–243.
<https://doi.org/10.1016/j.actaastro.2017.12.036>.
- [7] C.P. Mark, S. Kamath, Review of Active Space Debris Removal Methods, *Space Policy.* 47 (2019) 194–206.
<https://doi.org/10.1016/j.spacepol.2018.12.005>.
- [8] M. Shan, J. Guo, E. Gill, Deployment dynamics of tethered-net for space debris removal, *Acta Astronaut.* 132 (2017) 293–302.
<https://doi.org/10.1016/j.actaastro.2017.01.001>.
- [9] V. V Svotina, M. V Cherkasova, Space debris removal – Review of technologies and techniques . Flexible or virtual connection between space debris and service spacecraft, *Acta Astronaut.* (2022).
<https://doi.org/10.1016/j.actaastro.2022.09.027>.
- [10] A. Ledkov, V. Aslanov, Review of contact and contactless active space debris removal approaches, *Prog. Aerosp. Sci.* 134 (2022) 100858.
<https://doi.org/10.1016/j.paerosci.2022.100858>.
- [11] S. Kitamura, Large space debris reorbiter using ion beam irradiation, in: 61st Int. Astronaut. Congr. Prague, Czech Repub., 2010.
- [12] J.M. Ruault, M.C. Desjean, C. Bonnal, P. Bultel, Active Debris Removal (ADR): From identification of problematics to in flight demonstration preparation, in: 1st Eur. Work. Act. Debris Remov., 2010.
- [13] C. Bombardelli, J. Pelaez, Ion beam shepherd for contactless space debris removal, *J. Guid. Control. Dyn.* 34 (2011) 916–920.
<https://doi.org/10.2514/1.51832>.
- [14] C. Bombardelli, H. Urrutxua, M. Merino, E. Ahedo, J. Peláez, Relative dynamics and control of an ion beam shepherd satellite, *Adv. Astronaut. Sci.* 143 (2012) 2145–2157.

- [15] A.P. Alpatov, S.V. Khoroshylov, A.I. Maslova, Contactless de-orbiting of space debris by the ion beam. *Dynamics and Control, Akademperiodyka*, Kyiv, 2019. <https://doi.org/10.15407/akademperiodyka.383.170>.
- [16] A. Alpatov, S. Khoroshylov, C. Bombardelli, Relative control of an ion beam shepherd satellite using the impulse compensation thruster, *Acta Astronaut.* 151 (2018) 543–554. <https://doi.org/10.1016/j.actaastro.2018.06.056>.
- [17] S. Khoroshylov, Relative control of an ion beam shepherd satellite in eccentric orbits, *Acta Astronaut.* 176 (2020) 89–98. <https://doi.org/10.1016/j.actaastro.2020.06.027>.
- [18] V.M. Kulkov, N.N. Markin, Y.G. Egorov, Issues of controlling the motion of a space object by the impact of the ion beam, *IOP Conf. Ser. Mater. Sci. Eng.* 927 (2020). <https://doi.org/10.1088/1757-899X/927/1/012051>.
- [19] V.A. Obukhov, V.A. Kirillov, V.G. Petukhov, A.I. Pokryshkin, G.A. Popov, V.V. Svitina, N.A. Testoyedov, I.V. Usovik, Control of a service satellite during its mission on space debris removal from orbits with high inclination by implementation of an ion beam method, *Acta Astronaut.* 194 (2022) 390–400. <https://doi.org/10.1016/j.actaastro.2021.09.041>.
- [20] V. Aslanov, A. Ledkov, M. Konstantinov, Attitude dynamics and control of space object during contactless transportation by ion beam, *Proc. Int. Astronaut. Congr. IAC. 2020-October* (2020) 1–7.
- [21] V.S. Aslanov, A.S. Ledkov, Space debris attitude control during contactless transportation in planar case, *J. Guid. Control. Dyn.* 43 (2020) 451–461. <https://doi.org/10.2514/1.G004686>.
- [22] Y. Nakajima, H. Tani, T. Yamamoto, N. Murakami, S. Mitani, K. Yamanaka, Contactless space debris detumbling: A database approach based on computational fluid dynamics, *J. Guid. Control. Dyn.* 41 (2018) 1906–1918. <https://doi.org/10.2514/1.G003451>.
- [23] V. Aslanov, A. Ledkov, Detumbling of axisymmetric space debris during transportation by ion beam shepherd in 3D case, *Adv. Sp. Res.* (2021). <https://doi.org/10.1016/j.asr.2021.10.002>.

- [24] S. Kitamura, Y. Hayakawa, S. Kawamoto, A reorbiter for large GEO debris objects using ion beam irradiation, *Acta Astronaut.* 94 (2014) 725–735. <https://doi.org/10.1016/j.actaastro.2013.07.037>.
- [25] V.A. Obukhov, V.A. Kirillov, V.G. Petukhov, G.A. Popov, V.V. Svitina, N.A. Testoyedov, I.V. Usovik, Problematic issues of spacecraft development for contactless removal of space debris by ion beam, *Acta Astronaut.* 181 (2021) 569–578. <https://doi.org/10.1016/j.actaastro.2021.01.043>.
- [26] A. Barea, H. Urrutxua, L. Cadarso, Large-scale object selection and trajectory planning for multi-target space debris removal missions, *Acta Astronaut.* 170 (2020) 289–301. <https://doi.org/10.1016/j.actaastro.2020.01.032>.
- [27] M. Merino, Modeling the physics of plasma thruster plumes in electric propulsion, *ESAC Sci. Semin.* (2017). https://www.cosmos.esa.int/documents/13611/1287426/170126_Merino.pdf.
- [28] F.F. Gabdullin, A.G. Korsun, E.M. Tverdokhlebova, The Plasma Plume Emitted Onboard the International Space Station Under the Effect of the Geomagnetic Field, *IEEE Trans. Plasma Sci.* 36 (2008) 2207–2213. <https://doi.org/10.1109/TPS.2008.2004236>.
- [29] F. Cichocki, M. Merino, E. Ahedo, Spacecraft-plasma-debris interaction in an ion beam shepherd mission, *Acta Astronaut.* 146 (2018) 216–227. <https://doi.org/10.1016/j.actaastro.2018.02.030>.
- [30] IADC, IADC Space Debris Mitigation Guidelines, 3rd ed., 2021.
- [31] V.S. Aslanov, A.S. Ledkov, Fuel costs estimation for ion beam assisted space debris removal mission with and without attitude control, *Acta Astronaut.* 187 (2021) 123–132. <https://doi.org/10.1016/j.actaastro.2021.06.028>.
- [32] V.S. Aslanov, A.S. Ledkov, M.S. Konstantinov, Attitude motion of a space object during its contactless ion beam transportation, *Acta Astronaut.* 179 (2021) 359–370. <https://doi.org/10.1016/j.actaastro.2020.11.017>.
- [33] A. Alpatov, F. Cichocki, A. Fokov, S. Khoroshylov, M. Merino, A. Zakrzhevskii, Determination of the force transmitted by an ion thruster

- plasma plume to an orbital object, *Acta Astronaut.* 119 (2016) 241–251.
<https://doi.org/10.1016/j.actaastro.2015.11.020>.
- [34] J. Fisher, B. Ferraiuolo, J. Monheiser, K. Goodfellow, A. Hoskins, R. Myers, J. Bontempo, J. McDade, T. O'Malley, G. Soulas, R. Shastry, M. Gonzalez, NEXT-C Flight Ion System Status, in: *AIAA Propuls. Energy 2020 Forum*, American Institute of Aeronautics and Astronautics, Reston, Virginia, 2020: pp. 1–32. <https://doi.org/10.2514/6.2020-3604>.
- [35] M. Patterson, J. Foster, H. McEwen, D. Herman, E. Pencil, J. VanNoord, NEXT Multi-Thruster Array Test - Engineering Demonstration, in: *42nd AIAA/ASME/SAE/ASEE Jt. Propuls. Conf. & Exhib.*, American Institute of Aeronautics and Astronautics, Reston, Virginia, 2006: pp. 8187–8208. <https://doi.org/10.2514/6.2006-5180>.
- [36] J.-C. Liou, An active debris removal parametric study for LEO environment remediation, *Adv. Sp. Res.* 47 (2011) 1865–1876.
<https://doi.org/10.1016/j.asr.2011.02.003>.